

**Combined assessment of
drug dissolution and epithelial permeability:
Implementation of online TEER measurement
and extension to BCS class III and IV
compounds**

Dissertation

zur Erlangung des Grades

des Doktors der Naturwissenschaften

der Naturwissenschaftlich-Technischen Fakultät III

Chemie, Pharmazie, Bio- und Werkstoffwissenschaften

der Universität des Saarlandes

von

Marco Mündörfer

Saarbrücken

2010

Tag des Kolloquiums: 16.12.2010

Dekan: Prof. Dr. Stefan Diebels

Berichterstatter: Prof. Dr. Claus-Michael Lehr

Prof. Dr. Udo Bakowsky

Vorsitz: Prof. Dr. Gregor Jung

Akad. Mitarbeiter: Dr. Ulrich F. Schäfer

Die vorliegende Arbeit entstand auf Anregung und unter der Anleitung von

Herrn Prof. Dr. Claus-Michael Lehr

in Zusammenarbeit mit der

Sanofi-Aventis Deutschland GmbH

am Lehrstuhl für Biopharmazie und Pharmazeutische Technologie der

Universität des Saarlandes.

Abstract

Measurement of drug dissolution and permeation of solid oral dosage forms in a combined experiment is a quite obvious research approach that nevertheless has only been sparsely considered up to now. In the present work an existing apparatus that has been developed for the mentioned purpose has been adapted to comply with the requirements for the analysis of low permeable compounds of BCS classes III and IV. Next to that, the apparatus was developed further in a way that the course of transepithelial electrical resistance (TEER) could be recorded throughout conduction of an experiment. Implementation of this tool was supposed to provide for the opportunity to survey and demonstrate the integrity of a Caco-2 cell monolayer throughout an experiment. Furthermore, it was of interest to evaluate in how far the novel method was suitable for the analysis of the influences of excipients, as e.g. EDTA, on the permeability of the paracellular pathway. Finally, it was pointed out that the revised apparatus is able to analyze Lasix[®] 40mg furosemide tablets correctly. Hence, the research approach has advanced significantly to the aim of the establishment of an *in vitro* method for the targeted formulation development of low permeable compounds.

Zusammenfassung

Die Messung der Freisetzung und der Permeation von Arzneistoffen aus festen Darreichungsformen zur peroralen Anwendung in einem kombinierten Experiment ist ein naheliegender, bislang jedoch wenig behandelter Forschungsansatz. In der vorliegenden Arbeit wurde eine in einer vorangegangenen Arbeit zu diesem Zweck entwickelte Apparatur an die Erfordernisse zur Analyse von langsam permeierenden Substanzen der BCS Klassen III und IV angepasst. Weiterhin wurde die Apparatur dahingehend weiterentwickelt, dass der Verlauf des transepithelialen elektrischen Widerstandes während eines Versuches aufgezeichnet werden kann. Das Ziel dieser Maßnahme war es, die Prüfung der Integrität der Caco-2 Zellen, die in diesem Modell als Permeationsbarriere dienen, während eines Versuches zu ermöglichen. Daneben war es von Interesse zu untersuchen, inwieweit sich die neue Methode für die Analyse des Einflusses von Hilfsstoffen, wie beispielsweise EDTA, auf die Durchlässigkeit des parazellulären Transportweges eignet. Abschließend konnte gezeigt werden, dass die optimierte Apparatur bei der Analyse von Lasix[®] 40 mg Furosemid Tabletten, als Beispiel für eine BCS Klasse IV Substanz, korrekte Ergebnisse liefert. Somit ist der Forschungsansatz dem Ziel der Entwicklung einer *in vitro* Methode zur gezielten Formulierungsentwicklung von Problemарzneistoffen ein wesentliches Stück näher gekommen.

Acknowledgement

In the first place I want to thank Prof. Claus-Michael Lehr for giving me the opportunity to do this work under his supervision. I also want to thank him for his continuous support and encouragement as well as for valuable input in discussions and precedent-setting decisions.

Dr. Ulrich Schäfer was a contact person for me regarding various kinds of questions and I want to thank him for his advice in discussions, his persistency in his claims as well as for his support for the project in general throughout my time at the Department of Biopharmaceutics and Pharmaceutical Technology.

Dr. Balbach and Dr. Eichinger are thanked for their initiative to continue the co-operation between Sanofi-Aventis and Saarland University and the necessary financial support. Next to that I am grateful for their continuous company and interest in the project, for their courtesy and incitation as well as for critical reviews and remarks. I also want to thank Dr. Loos and Dr. Walk for the friendly and straight-forward contact and for their considerable effort and initiative to make the project a success.

At Saarland University I furthermore want to thank Mr. Ochs, the person in charge of precision engineering, for the realization of technical adaptations to the apparatus, and Mr. Skohoutil is thanked for support in electro technical matters.

Mr. Würtz and Mr. Klesen from the Department for Process Automation are thanked for their kind support in the adaptations necessary to allow a digital triggering of the measurement equipment for transepithelial electrical resistance.

Acknowledgement

Mr. Wolfhard Reimringer is thanked for support and introduction into LabVIEW software.

A big thank you goes to Petra König for her support in cultivation and maintenance of the Caco-2 cells, and to Leon Muijs for preparation of the microscope slides.

Thanks to Nico for the good times we spent as roommates at the institute, and thanks to all of the team at the department for a really nice atmosphere and a pleasant spirit of cooperativeness and kindness.

Thanks to Constanze for proofreading the thesis. But still more I want to thank her for her encouragement and patience as well as for listening and believing in me.

Finally, I want to thank my parents for their unconfined and confident support ever since I can remember.

Table of contents

1 Introduction.....	1
1.1 Introduction into dissolution and permeation measurement	1
1.1.1 Dissolution testing.....	1
1.1.2 Permeation assessment	4
1.2 Rational for the application of combined dissolution and permeation testing.....	8
1.3 Caco-2 cells as a surrogate for the intestinal barrier	10
1.4 Starting point of the PhD thesis	14
1.4.1 Proof of concept with the BCS class I compound propranolol HCl.....	15
1.4.2 Permeation of furosemide, a BCS class IV compound	16
1.5 Aims of this thesis	18
2 Adaptations of the apparatus for the analysis of BCS class III and IV drugs	20
2.1 Materials and methods	20
2.1.1 Caco-2 cell culture	20
2.1.2 TEER measurement	20
2.1.3 Buffer solutions and reagents	21
2.1.4 Sequential Injection Analysis	21
2.1.5 Apparatus for combined measurement of dissolution and permeation	21
2.1.6 Quantification of furosemide	22
2.1.7 Quantification of sodium fluorescein	24
2.1.8 Quantification of rhodamine 123	24
2.2 Case study with furosemide	25
2.2.1 Introduction	25
2.2.2 Permeation in the Transwell® setup	25
2.2.3 Permeation in the apparatus.....	30
2.2.3.1 Simplified basolateral conditions	33

2.3	Revision of the basolateral compartment.....	35
2.4	Hydrostatic pressure compensation between apical and basolateral side of the FTPC.....	37
2.5	Influence of automated sampling on permeation results.....	39
2.6	Test routine for SIA valves.....	42
2.7	Implementation of an independent route for basolateral sampling.....	46
2.8	Performance test of the revised apparatus.....	47
3	Online TEER measurement.....	49
3.1	Rationale for the implementation of online TEER measurement ...	49
3.2	Introduction into TEER measurement.....	50
3.2.1	TEER and tight junctions.....	50
3.2.2	Practical approaches for TEER measurement.....	51
3.3	Realisation of TEER measurement inside the FTPC.....	53
3.4	Proof of principle using analogue recording.....	55
3.5	Computer-controlled online TEER measurement.....	57
3.5.1	Adaption of the EVOMX.....	57
3.5.2	Computer-controlled measurement.....	57
3.6	Lifetime of Caco-2 cells inside the FTPC.....	58
3.7	Microscopic inspection of Caco-2 cells in comparison to TEER measurement.....	61
3.8	Online TEER measurement as a tool for the analysis of the influence of excipients on cell monolayer permeability.....	63
3.8.1	Introduction.....	63
3.8.2	Buffer solutions.....	64
3.8.3	Experimental procedure.....	65
3.8.4	Results.....	65
3.8.5	Recovery of TEER after repeated Ca ²⁺ switching.....	67
3.8.6	Discussion.....	68
3.8.7	Conclusions.....	70
4	Proof of concept using the BCS class IV compound furosemide.....	72
4.1	Permeation of furosemide in the revised apparatus.....	72

5 Summary and outlook	76
6 Annexes.....	78
6.1 List of abbreviations	78
6.2 Allocation of the ports at the SIA valves	80
6.2.1 8-port valve	80
6.2.2 6-port valve	80
6.3 Programming codes for SIA automation.....	81
6.3.1 SIA programs for furosemide	81
6.3.2 SIA programs for fluorescein and rhodamine.....	84
6.3.3 Test routine for the multiposition-valve	87
6.4 Autosampler configuration.....	89
6.5 PEEK adapter for electrode plugs	90
7 Curriculum vitae	91
8 List of publications.....	92
9 References	93

1 Introduction

1.1 Introduction into dissolution and permeation measurement

1.1.1 Dissolution testing

Dissolution testing of oral dosage forms has become a standard method in pharmaceutical quality control and formulation development since its introduction into the USP in 1968. The dissolution profile, primarily assessed in apparatus 1 or 2 USP, is a major characteristic of a marketed drug product. It is relevant for registration, batch release and represents an indicator for the suitable performance of the whole manufacturing process as well as for consistent product quality. With the introduction of the Biopharmaceutical Classification System (BCS) categorizing compounds according to their solubility and permeability into four groups (Table 1-1), the scientific basis for a further increase of the significance of dissolution testing was provided [1, 2]. The increase of knowledge, expanded in broad scientific discussions, provided the basis for the regulatory authorities to establish a legislation that allowed the granting of biowaivers for immediate release (IR) products of BCS class I compounds [3]. This concept stipulated that for compounds featuring a high aqueous solubility at a physiological range of pH and a high intestinal permeability (BCS class I) the account for bioequivalence studies may be waived. From a scientific point of view it was evident that in such cases a failure of an IR drug product *in vivo* can only be associated with a mistake in the pharmaceutical formulation leading to a delayed or incomplete release of the active pharmaceutical ingredient. To exclude such issues standardized dissolution testing was regarded as an adequate, efficient and sufficiently significant *in vitro* method. Furthermore, it seems to be evident that along with increasing *in vivo* relevance of the dissolution data, e.g. by application of biorelevant dissolution media, the potential significance of dissolution

testing in respect to drug product quality associated questions is not yet bailed out [4].

Class I Solubility: high Permeability: high	Class II Solubility: low Permeability: high
Class III Solubility: high Permeability: low	Class IV Solubility: low Permeability: low

Table 1-1 The BCS categorizes compounds according to the parameters solubility and permeability into four classes.

A further area of research that is closely linked to dissolution testing is the establishment of *in vitro* - *in vivo* correlations. Here, it is aimed to elucidate an interconnection between the *in vivo* drug profiles obtained in small pharmacokinetic studies and a physicochemical property of oral drug formulations which in most cases will be represented by the dissolution profile [5]. If such correlations are available, bioequivalence studies may be waived if for example an intermediate dosage strength is supposed to be marketed or if small changes in the formulations have to be conducted. Once established, an IVIVC can be used in such cases to provide sufficient evidence for the expected *in vivo* performance only analyzing the dissolution profile of the new product. Not for all compounds it is likely that an IVIVC can be found. E.g. in the case of BCS class III compounds, featuring a permeation rate limited absorption, an IVIVC cannot be expected, as any difference in the dissolution properties of formulations will be levelled by the slow overall permeation of the drug. So, in general, it is only reasonable to look for a dissolution based IVIVC if the permeation is not the rate limiting step, as in this case it can be supposed that differences in the dissolution properties of formulations are reflected in the *in vivo* drug absorption. In this context combined measurement of

dissolution and permeation can be useful to obtain more significant IVIVCs using the *in vitro* permeation after a preceding dissolution step as the most obvious parameter for correlation with the *in vivo* pharmacokinetic data [6]. Apart from that, BCS class III compounds provide further interesting discussions. The question is if for such compounds, showing a sufficiently high aqueous solubility in the range of pH 1.0 to pH 7.5, it is necessary to insist on bioequivalence studies e.g. for market authorisation of generics. As already explained, in such cases permeation of the solute drug molecules across the intestinal barrier is supposed to be the rate limiting step in the absorption process. So, applying the principles of BCS no significant differences between oral IR products are to be expected as long as the dissolution is very rapid (85% release within 30 min at pH 1.2, 4.5 and 6.8). Therefore, the discussion about granting of biowaivers also for e.g. BCS class III compounds on the basis of results from dissolution testing appears to be quite reasonable [7-9]. Next to this BCS class III attributed point of discussion several further proposals to expand the legislation of the granting of biowaivers as e.g. the inclusion of IR formulations of weak acids categorized as BCS class II and soluble in 250 ml at pH 6.8. [10-12]. The most well founded and broadly accepted approaches have been picked up in a WHO proposal which was supposed to allow waiving the account for *in vivo* BE studies of solid oral IR dosage forms of many APIs mentioned on the WHO model list for essential medicines [13]. This proposal included a revision of the criteria for BCS classification narrowing the pH window for high solubility to pH 1.2 – 6.8. Also the requirement for the status of high permeability was relaxed from formerly 90% to 85% absorption shifting some compounds that formerly were considered as BCS class III to class I. This document was adopted by the WHO expert committee on specification of pharmaceutical preparations. Thereby, the guideline provides recommendations for the authorities in charge of the approval of generic pharmaceutical products,

which are actualized to current scientific knowledge [14]. In context with growing knowledge about the impact of drug metabolism and transport a modification of the BCS called Biopharmaceutical Drug Disposition Classification System (BDDCS) was proposed [15]. In this concept the BCS parameter permeability was proposed to be replaced or extended by designation of the major route of drug elimination. In case of metabolism as the major route of drug elimination the compound would be regarded as highly permeable while in case of predominant renal or biliary excretion of unchanged drug it should be classified as low permeable. With application of > 90% metabolized as the cut-off criterion for high permeability next to the criterion of > 90% absorption, postulated by the BCS, the number of compounds assignable to BCS class I would be significantly enlarged. Finally, this concept would allow a broader application of biowaiver decisions based on metabolism [16]. So, it is evident that the efforts to illuminate the biopharmaceutical interrelations and the refinement and standardisation of *in vitro* methods will have to be prosecuted in order to minimize redundant human clinical studies and facilitate access to reliable and affordable medicines in developing countries.

1.1.2 Permeation assessment

The method of choice for intestinal permeation assessment that is suitable for classification of a compound according to the BCS is the determination of the extent that is absorbed in humans, which can either be performed as a mass balance or as a comparison to an intravenous reference dose [1, 2]. According to the original BCS guideline compounds showing an absorption of at least 90% are considered as highly permeable. Results from animal testing, especially using the *in situ* intestinal perfusion method in rats, are often considered as the number-two choice. Whereas

conformity between rat and man could not be found for the total bioavailability and comparing the expression levels of metabolizing enzymes, correlations for the intestinal permeability ($R^2 = 0.8$) and moderate correlation for the expression levels of drug transporters ($R^2 > 0.56$) have been reported [17, 18]. Therefore, it can be concluded that the significance of the animal data is not necessarily higher than that obtained by *in vitro* permeation measurement. In an *in vitro* approach, the permeability of compounds can either be measured across biological barriers consisting of viable cells [19, 20], or across artificial membranes [21]. Whereas the basic mechanism underlying the models using artificial membranes is passive diffusion through the membrane material and the surrounding unstirred layers, the biological models are closer to the *in vivo* situation. Next to the availability of a transcellular and a paracellular pathway, those models also include mechanisms of active influx and efflux transport as well as intracellular enzymatic metabolism (Figure 1-1).

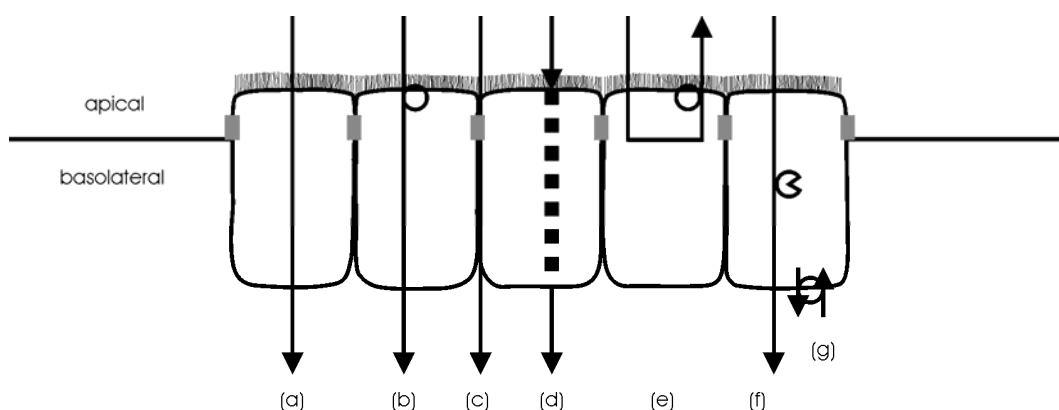


Figure 1-1 Pathways and mechanisms of transport across small intestinal cells: (a) passive transcellular transport by diffusion into and out of the cell; (b) active uptake followed by passive diffusion; (c) passive paracellular transport governed by the permeability of the tight junctions; (d) transcellular vesicular transport (transcytosis); (e) passive transcellular uptake followed by active apical efflux transport; (f) passive transcellular transport modified by enzymatic metabolism; (g) basolateral active transport (in- and efflux).

The biological models can be further subdivided into native tissue that has been excised from an organism or tissue that has been grown using cell culture technique. In general it can be said that the tissue originating from cell culture is less viable and robust as its native counterpart. On the other hand it features the significant advantage of containing no ethical conflicts which makes cell culture technology to an important branch of methodologies to realize the goals of the 3R concept, which is more than ever up to date [22]. In the practical approach, small intestinal tissue of rats is mounted in an Ussing chamber in order to determine the effective permeability (P_{eff}). Good correlation ($R^2 = 0.95$) between P_{eff} in man, derived from *in vivo* data, and P_{eff} values across rat intestinal tissue have been observed, although on an absolute scale the permeability in humans was 5 to 6 fold higher [23]. It was speculated that these differences could partly be explained by the lack of blood flow in the rat *in vitro* experiments. Apart from predicting human permeability the Ussing chamber model e.g. allowed revealing differences in the permeation rates in different intestinal regions of the rat [24]. The most widely used approach for permeation measurement across artificial barriers is the parallel artificial membrane permeability assay (PAMPA) first described by Kansy et al [25]. It is based on the 96 well scale allowing a high degree of automation and uses phospholipid coated Polyvinylidene fluoride (PVDF) filter membranes as permeation barrier. This approach by Hoffmann La-Roche attracted great attention in the pharmaceutical industry and was followed by the development of similar PAMPA approaches by other pharmaceutical companies. One of the critical points in this methodology was the discord of the best source for the initially used lecithin and its generally low degree of standardization. Therefore, Avdeef and coworkers developed an optimized coating containing Dioleoyl-sn-glycero-3-phosphocholine (DOPC) instead of lecithin and further improved the method, e.g. by introduction of a pH gradient and a lipophilic gradient which was called the “Double-Sink”

PAMPA model [21]. Today, PAMPA which is suitable for automated high throughput screening and permeability measurement over Caco-2 cells have become standard methods in the early development of new APIs. Both methods provide complementary results and allow well substantiated conclusions about the presumable performance in humans. Regarding the apparatus for combined measurement of dissolution and permeation it is favourable to use a model that comes as close as possible to the original intestinal barrier in order to obtain the maximum *in vivo* relevance of the experimental data. Furthermore, the model should allow evaluating the interplay of excipients or the drug itself with transporter proteins and enzymes. At the moment these requirements are met best by the Caco-2 cell model although it is well known that it does not mimic the small intestinal barrier perfectly [26]. A comparison of the relevant cell culture models can be found in chapter 1.3. Nevertheless, the option of an artificial membrane inside the FTPC would be advantageous as it e.g. allows studying the contribution of passive permeation to overall permeability.

1.2 Rational for the application of combined dissolution and permeation testing

A major limitation for the development of new drugs is the often encountered and ever increasing issue of poor oral bioavailability of drug candidates detected in high throughput screening [27]. In consequence, the pharmaceutical industry faces the situation that an increasing number of compounds in the pipelines for small molecule development belong to BCS classes III and IV. These compounds share an intrinsic low permeability which is difficult to address. In case of BCS class IV, classical galenical approaches like micronization, preparation of solid solutions or microemulsions may be useful if the compound of interest is very lipophilic and features a dissolution rate limited absorption [28]. For larger and more hydrophilic compounds the mentioned galenical approaches will probably not be sufficient as in those cases permeation across the intestinal epithelium governs the overall absorption. Therefore, there is a keen interest in the finding and registration of suitable excipients increasing the intestinal permeability in man. Although over the years a lot of articles proposing a variety of compounds for such purposes have been published, only very few examples, like e.g. tocopheryl polyethylene glycol succinat (TPGS) in Agenerase[®], have found their way into a marketed product. Another example is the concomitant application of 100 mg ritonavir as a booster of the pharmacologic effect of other protease inhibitors which is based upon the strong inhibition of mainly CYP 3A4 based metabolism of protease inhibitors by ritonavir [29]. A major reason for the lack of application of classical permeation enhancers is the significant toxicity which in most cases is linked with a high efficiency of an enhancer. Lately, a systematic approach analyzing a variety of 51 enhancers from 11 distinct chemical groups in a standardized procedure focusing on the relationship of toxicity and potency was published [30]. In this study several excipients

that have been reported to comprise permeation enhancing properties but have not been in the focus of research up to now were shown to be effective without significant toxicity. In a second study the authors were able to point out synergistic effects applying a combination of up to three very potent excipients at low, nontoxic doses [31]. These studies demonstrate the high potential of excipients for permeation enhancement via the enteral route and encourage for further research with the most promising compounds in a more realistic approach, e.g. applying complete oral formulations containing excipients and a model drug. In this context the apparatus is the ideal means to bridge the gap between 96 well based approaches and *in vivo* pharmacokinetic studies, as it is specially designed for performance testing of complete oral dosage forms, thereby representing an *in vitro* tool to test and optimize novel formulation approaches. So, the determination and dosing of the ideal enhancer or combination of enhancers for an individual API might be performed using the apparatus minimizing the need for *in vivo* studies.

1.3 Caco-2 cells as a surrogate for the intestinal barrier

Since its isolation from human colon adenocarcinoma tissue in 1977 Caco-2 cells have become a well characterized and widely used model for the small intestinal epithelium [32, 33]. In pharmaceutical development analysis of Caco-2 cell permeability has become a standard method to estimate human absorption of new compounds and the cell line is routinely applied to screen a compound for affinity to intestinal active transporters [34-36]. Furthermore, Caco-2 cells find frequent application to study gut wall associated metabolism and toxicity [37, 38]. The high acceptance of the Caco-2 cell model as a surrogate for the small intestinal barrier can be explained by its physiological similarity to the native human epithelium and visualizing its singularities and advantages over other approaches. Having reached confluence Caco-2 cells spontaneously differentiate into an enterocyte typic phenotype with the formation of brush border associated microvilli as the most definite sign of apical and basolateral polarisation [39]. Along with the expression of functional tight junctions this habit was found to be maintained also after growing the cells on permeable supports which allowed conducting transport studies across Caco-2 cells [32]. Several studies pointed out good correlations between Caco-2 cell permeability and human intestinal absorption [17, 40-43]. The presence of the most important active transporters e.g. MCT1, PepT1 and OATP-B as well as efflux pumps like MDR1 (P-gp), MRP2 and BCRP was demonstrated suggesting the Caco-2 cell model as a tool to analyze the uptake mechanism of compounds and relative expression levels of these proteins were found to correlate with those of human intestinal epithelium. Nevertheless, smaller absolute levels of expression for some transporters like PepT1 and BCRP should be considered [44, 45]. In practical application the Caco-2 model revealed active transport or efflux for a variety of compounds, pointing out the significance of these mechanisms

in the overall absorption process [46]. A further topic that stays in the focus of research is epithelial and hepatic drug metabolism. Caco-2 cells express a variety of metabolic enzymes, but CYP3A4, the enzyme that is responsible for the metabolism of the majority of marketed compounds is expressed only weakly or not at all. Here, the induction of the gene by vitamin D3 or transfection of the cells with the CYP3A4 gene paved way to study the interplay of metabolism and efflux transport [38, 47-49]. But despite those approximations and similarities one should be aware that there are still notable differences between original human intestinal tissue and Caco-2 cells. A general drawback in comparison to excised tissue is the lesser robustness and vitality of cell culture models. Furthermore, native intestinal epithelial tissue is composed of two different cell types: ciliated cells and mucus producing goblet cells. Caco-2 cells are derived from ciliated cells and therefore the model does not feature a mucus layer. This mucus layer might be of relevance for intestinal drug absorption as it provides a pH gradient between lumen and cell surface which seems to be maintained by restricted diffusion of H⁺ ions secreted by the epithelial cells [50]. Direct measurement of the pH at the mucus layer with pH-microelectrodes revealed a range of pH 5.8 to 6.3 in rat [51]. In order to account for the influence of the jejunal pH-microclimate the application of slightly acidic apical donor solutions of pH 6.0 was proposed [52]. Co-culture approaches of Caco-2 cells and the mucus producing goblet type cell lines HT-29-H and HT29-MTX were established but did not yield sufficiently close approximation to the physiological conditions to compensate the additional work and expenses in contrast to Caco-2 cell monocultures [53, 54]. Intact Caco-2 cell monolayers feature higher TEER values and a generally less leaky paracellular barrier than native human intestinal tissue which might be attributed to the colonic origin of the cell line [33]. This correlates to the finding that rather hydrophilic drugs which are primarily absorbed via the paracellular route show lower permeability

in the Caco-2 model in comparison to humans [40]. In general it was shown that the predictive value of the Caco-2 cells for low permeable compounds is smaller than for high permeable compounds [55]. In this context the recently introduced 2/4/A1 cell line, originating from human small intestinal cells, was proposed as an alternative to study the permeation of passively absorbed drugs as it seemed to mimic the paracellular barrier better than the Caco-2 cells which e.g. manifested in lower, more physiologic TEER values below $100 \Omega \times \text{cm}^2$ [56]. Great interest has been devoted to the determination of the paracellular pore size which can be calculated from the permeation data of marker compounds using the Renkin molecular sieving function or analyzing the permeability of a series of PEG molecules to determine the cut-off molecular radius. Those data from different laboratories were re-evaluated recently using consistent input parameters suggesting a range of 4.0 to 12.9 Å for the paracellular pore size in unperturbed Caco-2 cell monolayers and a pore size of 17.8 Å for the 2/4/A1 cells line [57]. A recent study analyzing the permeability of different cell lines in comparison to human jejunal patches reported a biphasic permeability for Caco-2 cells and human intestine with nearly identical pore sizes and a monophasic permeability for the 2/4/A1 cells with a pore size of 14.9 Å. Therefore, the authors concluded that the known difference between paracellular permeability between Caco-2 cells and human small intestine might be ascribed to a lower pore density in the Caco-2 cell monolayers. Concerning the 2/4/A1 cells the authors supposed different paracellular permeation properties which raises questions about the previously postulated superiority of this novel cell line. Considering the purposes that the apparatus for combined measurement of dissolution and permeation has been developed for, the Caco-2 cell monolayer provides the most suitable cell culture model for the intestinal barrier at this moment. Due to the strong expression of efflux transporters it allows to evaluate performance testing of oral dosage forms containing

P-gp inhibitors incorporated into the drug formulation. Recently, the usefulness of TEER measurement to point out effective permeation enhancement with Caco-2 cell monolayer has been demonstrated [30]. So, also in the case of deliberate affectation of the tight junctions to obtain permeation enhancing effects, the Caco-2 cell model is very useful maybe even because it features higher TEER and a tighter paracellular barrier than human small intestinal tissue. Nevertheless, it could be useful to implement a CYP3A4 competent Caco-2 cell line in order to also study the influences of metabolism. Certainly, the ongoing research on the novel 2/4/A1 cell line should be followed critically, as implementation of this human small intestinal cell line might become an option to maximize the *in vivo* relevance if a higher predictive value for low permeable compounds can be confirmed. Finally, the major drawback of the Caco-2 cell model, which can partly be assigned to the dynamic growth of research on this cell line should also be mentioned. It is the low level of standardisation of experimental procedures and protocols hampering the comparability of results from different laboratories and leading to significant interlaboratory differences that prevent the Caco-2 model from an even higher reputation. In order to improve this situation and strengthen the argumentation for *in vitro* cell culture models as a reliable substitute of *in vivo* studies, several efforts to pave way for a better standardisation of the model have been conducted in the last years [58-61].

1.4 Starting point of the PhD thesis

In a first PhD thesis, from 2004 to 2007, Stephan Motz developed the theoretical and practical basis for the combined assessment of dissolution and permeation using solid oral dosage forms [62]. At that time three interesting approaches had already been described in the literature. In 1999 Ginski and Polli published a simple continuous dissolution / Caco-2 permeability setup that allowed prediction of the dissolution / absorption relationship in an *in vitro* experiment [63]. Using immediate and extended release formulations of three compounds belonging to different classes of the BCS the setup enabled to illustrate the differences in the oral bioavailability between dissolution- and absorption rate limited drugs absorption. Using the example of Piroxicam, a BCS class II compound, the authors demonstrated a switch from dissolution rate limited permeation for the extended release formulation to a permeation rate limited pattern when the immediate release formulation was tested. One major drawback of Ginski and Polli's approach was that dissolution took place in a closed vessel, similar to apparatus 2 USP (rotating paddles). This resulted in a continuously increasing drug concentration on the donor side over time which is not in agreement to the physiological scenario of increasing and dropping gastrointestinal drug concentrations. In another approach published by Miyazaki and co-workers, however, this was improved using a flow through dissolution vessel and thereby applying an open system [64]. But the low flow rate in the dissolution module may limit the use of this setup for the application of complete oral dosage forms. A third approach by Kataoka and coworkers used a custom made side-by-side diffusion cell with a Caco-2 cell monolayer mounted in between [65]. An advantage of this system is its technical simplicity but on the other hand the approach is limited by the small apical volume which is available for dissolution and its character of a closed system similar to the approach by

Ginski and Polli. For a detailed depiction and analysis of the mentioned approaches for combined measurement of dissolution and permeation the reader is referred to the introductory chapter of Mr. Motz's thesis [62]. In order to allow the analysis of complete solid oral dosage forms the apparatus developed at the Saarland University therefore features a compendial flow through dissolution cell (apparatus 4 USP) upstream the permeation module. This setup warrants an *in vivo* like situation of drug release and provides the basis for the design of the apparatus as a tool for advanced *in vitro* formulation development.

1.4.1 Proof of concept with the BCS class I compound propranolol HCl

After development of the apparatus its performance was tested using propranolol HCl immediate and extended release formulations. It was shown that the single components of the setup like stream splitter, pumps and the FTPC provided consistent and reproducible results. For propranolol tablets a total amount of approximately 0.35% of the apically offered drug permeated over the Caco-2 monolayer into the basolateral compartment [62]. Furthermore, dose linearity could be pointed out. Regarding the analysis of propranolol ER tablets, differences in the dissolution profile in contrast to the IR formulations had only a small impact on the overall permeation culminating in a value of approximately 0.38% of the offered dose for a formulation containing 8% Eudragit® NE 30D. In a second step an automation of sampling and detection was provided by installation of components for Sequential Injection Analysis (SIA) a further development of Flow Injection Analysis (FIA) [66]. In summary, propranolol HCl was a suitable compound to test the apparatus' practical application and to perform a proof of concept study for the

combined measurement of dissolution and permeation of solid oral dosage forms. The major reasons for the choice of the compound were its unproblematic ADME parameters reflected in its categorization as a BCS class I compound. In general, it was necessary to analyse a BCS class I compound as a high permeability marker estimating the upper limit of permeation in the apparatus and evaluating the performance of the individual components of the setup. Only afterwards the analysis of low permeable compounds was sensible.

1.4.2 Permeation of furosemide, a BCS class IV compound

As a suitable compound for pointing out the benefits of combined measurement of dissolution and permeation, furosemide, a BCS class IV compound [67] was chosen. Next to its unfavourable physicochemical properties the compound showed asymmetrical transport across Caco-2 cell monolayers suggesting that it is a substrate of an efflux pump [54, 62, 68, 69]. Initial experiments with the marketed Lasix[®] 40mg IR tablet using a Sotax CE1 pump which generates a turbulent flow inside the dissolution module yielded a quick and complete release of the compound within two hours. The cumulative amount of furosemide that was detected at sampling port B reached 0.577% of the amount that was measured at the apical side which is rather high considering the results for propranolol as a high permeable drug, yielding a cumulative permeation of approximately 0.35% [62]. Several potential reasons had already been excluded at that point of time including leakage of the FTPC and disruption of the Caco-2 cell monolayer but the reason for the high permeability of furosemide remained unknown. Therefore, it was necessary to conduct a deeper study concerning the permeation of furosemide as a next step. This was considered to be an essential point and an urgent matter of research, as

the application of the apparatus will only offer its full value in the case of permeation rate limited drug absorption. In such cases effects taking place at the epithelial barrier like oversaturation of active transporters or the influence of excipients on efflux transport, drug metabolism or paracellular permeability gain in importance and may be crucial for the overall extent of drug absorption. As a precondition to analyze such phenomena the apparatus has to be able to pick up the results for the permeation of low permeable compounds correctly.

1.5 Aims of this thesis

The first aim of the work was to enable the apparatus to measure low permeable compounds. Due to the unexpectedly high permeation of furosemide the performance of the compound inside and outside of the apparatus should be analyzed. Based on the results it should be clarified if the apparatus in its present form was suitable to study low permeable compounds or if it had to be adapted.

After the apparatus had proven to pick up the permeation of low permeable compounds correctly it was aimed to focus on studies pointing out the benefit of combined measurement of dissolution and permeation over single dissolution or permeation assessment. Therefore, the effect of P-gp inhibitors like Tween 80 and TPGS which should be coadministered to the furosemide tablet should be studied. Due to the amphiphilic character of these compounds potential effects on dissolution were conceivable as well, making these excipients interesting candidates for formulation development of BCS class III and IV compounds.

When this project was started, a feedback about the status of the Caco-2 cell monolayer could only be obtained before and after conduction of an experiment as there was no access to the cell monolayer as soon as it was mounted inside the FTPC. This situation was considered as not sufficient and therefore it was intended to implement a tool to monitor the cell monolayer throughout conduction of an experiment. As a suitable method online measurement of Transepithelial Electrical Resistance (TEER) should be implemented inside the FTPC and its suitability to point out the cell monolayer integrity throughout the whole time of an experiment should be evaluated.

Next to the purpose of quality assurance, it should be evaluated if online TEER measurement was a suitable tool to analyze effects of formulation excipients upon the paracellular integrity of a Caco-2 cell monolayer. In this case online TEER measurement could be a valuable tool for advanced *in vitro* formulation development and provide a rationale for the deliberate application of e.g. permeation enhancers to solid oral dosage forms.

2 Adaptations of the apparatus for the analysis of BCS class III and IV drugs

2.1 Materials and methods

2.1.1 Caco-2 cell culture

Caco-2 cells, clone C2BBE1, were purchased at passage 60 from American Type Culture Collection (ATCC; Manassas, VA; USA) and used at passages 65-78. Cells were grown in T-flasks (75 cm²) at a temperature of approximately 37 °C in a humidified atmosphere containing approximately 5% CO₂. Cell culture medium was changed every second day and consisted of Dulbecco's Modified Eagle's Medium (DMEM) supplemented with 10% fetal calf serum (FCS) and 1% non-essential amino acids (NeAA). At approximately 90% confluence cells were trypsinated and seeded on Transwell[®] permeable supports (Transwell[®] type 3460, Corning Inc., Acton, MA, USA) in a density of 60,000 cells/cm². Transwell[®] supports were used for experiments after 21-25 days post seeding.

2.1.2 TEER measurement

Transepithelial electrical resistance (TEER) of the Caco-2 cell monolayers was measured with an EVOMX and handheld STX-2 electrodes (World Precision Instruments, Sarasota, FL, USA) before and after an experiment. The resistance of the blank permeable support was subtracted.

2.1.3 Buffer solutions and reagents

Krebs Ringer Buffer (KRB) consisting of 1.41 mM CaCl₂, 2.56 mM MgCl₂, 3.00 mM KCl, 142.03 mM NaCl, 0.44 mM K₂HPO₄, 4.00 mM D- Glucose and 10.0 mM HEPES adjusted to pH 7.4 was used as donor and acceptor medium. All salts for KRB preparation were of cell culture tested grade and obtained by Sigma Aldrich. Furosemide and propranolol HCl pure substances were obtained from Fagron (Barsbüttel, Germany).

2.1.4 Sequential Injection Analysis

Components for automation of the apparatus for combined measurement of dissolution and permeation consisted of a FIALab 3500 (FIALab instruments, Bellevue, WA), an autosampler (Cetac ASX 260, Omaha, NE, USA), an USB 2000 UV-Vis spectrometer and a D 2000 light source (Ocean Optics, Dunedin, FL, USA). The light source and the spectrometer were linked with a SMA Z-Flow Cell (Teflon[®], 5 mm optical path length) for flow through absorption measurement with two fibre optic cables. Spectrometer settings and program codes can be found in chapter 6.3.

2.1.5 Apparatus for combined measurement of dissolution and permeation

At the beginning of the studies the apparatus was composed analogue as described in detail by Mr. Motz [62] and depicted in a schematic overview in (Figure 2-1).

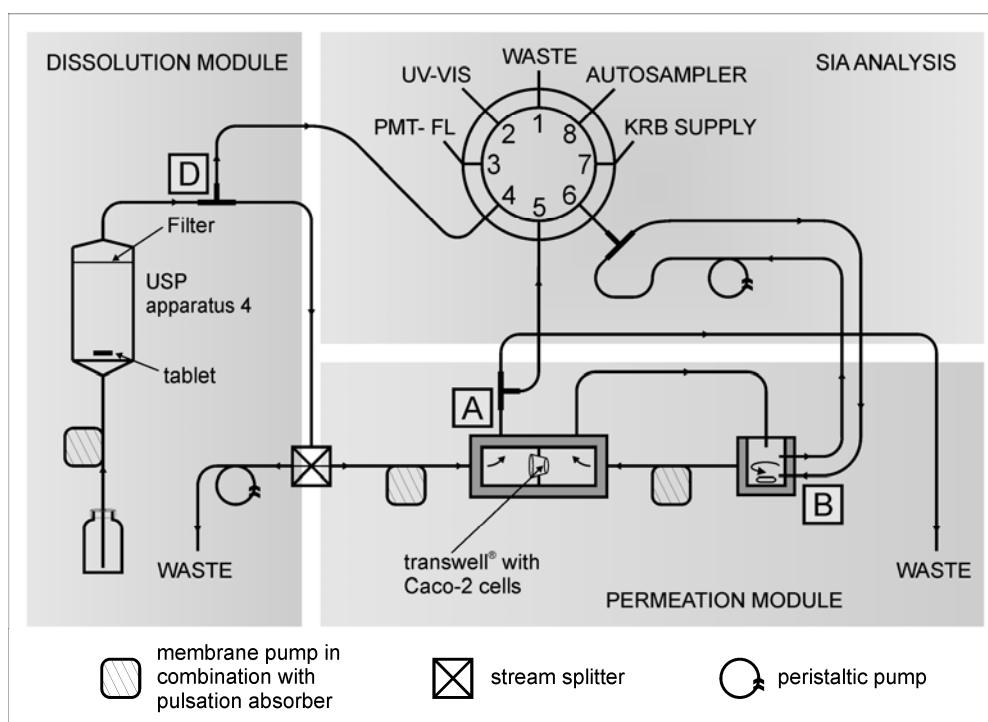


Figure 2-1 Schematic depiction of the automated apparatus for simultaneous measurement of dissolution and permeation. Sampling ports are indicated with capital letters, D for Dissolution, A for Apical and B for Basolateral. The multiposition valve and its port assignment was as follows: Port 1 was connected with the waste, port 2 with the UV-Vis detector, port 3 with the fluorescence detector (PMT-FL), port 7 was connected to the KRB supply for replenishing the volumes taken from the basolateral compartment. Port 8 was connected to the autosampler for aspirating the standard solutions and filling of basolateral samples into HPLC vials. Ports 4, 5 and 6 are assigned to sampling ports D, A and B, respectively.

2.1.6 Quantification of furosemide

Furosemide was quantified using a Dionex UltiMate 3000 HPLC system consisting of a Dionex ISO-3100A pump, a Dionex WPS-3000 TSL autosampler, a Dionex VWD-3400 variable wavelength detector, a Dionex TCC-3000 column compartment and a Dionex SRD-3200 solvent rack. A RP 18 column (LiChroSpher® 100, Merck) 5 µm, 12.5 cm was

implemented and the HPLC was run on Chromeleon software version 6.80 SP2 build 2284. The mobile phase consisted of 60% water (v/v), 30% acetonitrile (v/v), 10% methanol (v/v), 0.033% triethylamine (v/v) and 0.044% phosphoric acid (v/v). The flow rate was set to 1.2 ml/min, the temperature of the column oven was adjusted to 40 ± 1 °C and the wavelength for furosemide detection was set to 235 nm. Retention time was $3.02 \text{ min} \pm 0.04 \text{ min}$. It was shown that neither the matrix of KRB nor the excipients of the tablets interfered with the analysis.

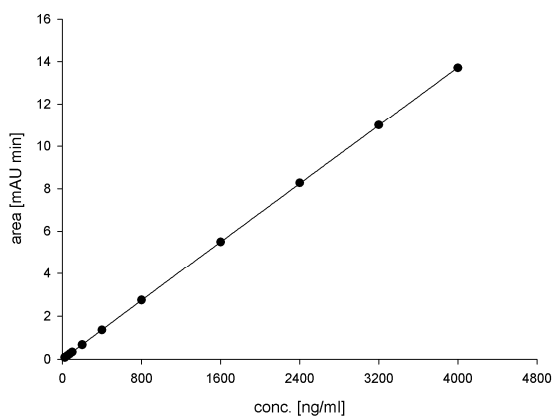


Figure 2-2 Calibration line for furosemide using described HPLC method.

Calibration was linear ($R^2 > 0.9999$) in the range of 25 – 4000 ng/ml. The slope of the calibration line was 3.425 ± 0.017 and the offset was calculated as -0.0044 ± 0.0047 . LOD was determined as 0.007 ± 0.001 µg/ml and LOQ was determined as 0.018 ± 0.007 µg/ml. Both parameters were calculated based on the residual standard deviation and the slope as recommended in ICH Q2 (R1) guideline.

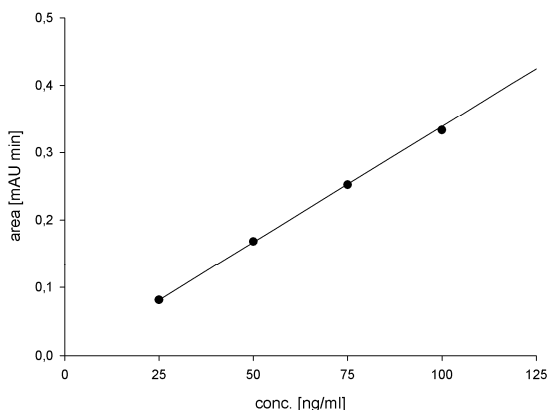


Figure 2-3 The figure shows an excerpt of the calibration line for furosemide showing the lower concentrations of the standards.

2.1.7 Quantification of sodium fluorescein

For quantification of sodium fluorescein in 96 well plates a Cytofluor II fluorescence reader was used ($\lambda_{\text{exc}} = 485 \text{ nm}$, $\lambda_{\text{em}} = 530 \text{ nm}$), (PerSeptive Biosystems, Wiesbaden-Norderstedt, Germany). Linearity ($R^2 > 0.999$) was ensured between 5 ng/ml and 1 $\mu\text{g/ml}$.

2.1.8 Quantification of rhodamine 123

For quantification of Rhodamine 123 in 96 well plates a Cytofluor II fluorescence reader was used ($\lambda_{\text{exc}} = 485 \text{ nm}$, $\lambda_{\text{em}} = 530 \text{ nm}$), (PerSeptive Biosystems, Wiesbaden-Norderstedt, Germany). Linearity ($R^2 > 0.999$) was ensured between 4 ng/ml and 0.2 $\mu\text{g/ml}$.

2.2 Case study with furosemide

2.2.1 Introduction

After successful measurement of propranolol HCl IR and ER formulations it was aimed to evaluate the eligibility of the apparatus also for low permeable compounds of BCS classes III or IV. Initial results with furosemide, a BCS class IV compound, yielded a fairly high permeation, which was even higher than for the high permeable compound propranolol. So the study of this topic was regarded as an urgent matter of research as the option to analyze low permeable compounds is a prerequisite for the reasonable application of the apparatus in successive studies. First questions that were arising were if the phenomenon was linked with the compound itself or with the apparatus. To clarify this, the permeation of furosemide was analyzed in two surroundings, the Transwell® setup and the apparatus.

2.2.2 Permeation in the Transwell® setup

Initial experiments were conducted outside of the FTPC in the Transwell® system in order to analyze the permeation patterns of furosemide under standardized conditions. As can be seen in Figure 2-4 the drug permeated linearly across Caco-2 cell monolayers after application of 200 µg/ml, 500 µg/ml and 1000 µg/ml furosemide donor solutions in the apical compartment.

Adaptations of the apparatus for the analysis of BCS class III and IV drugs

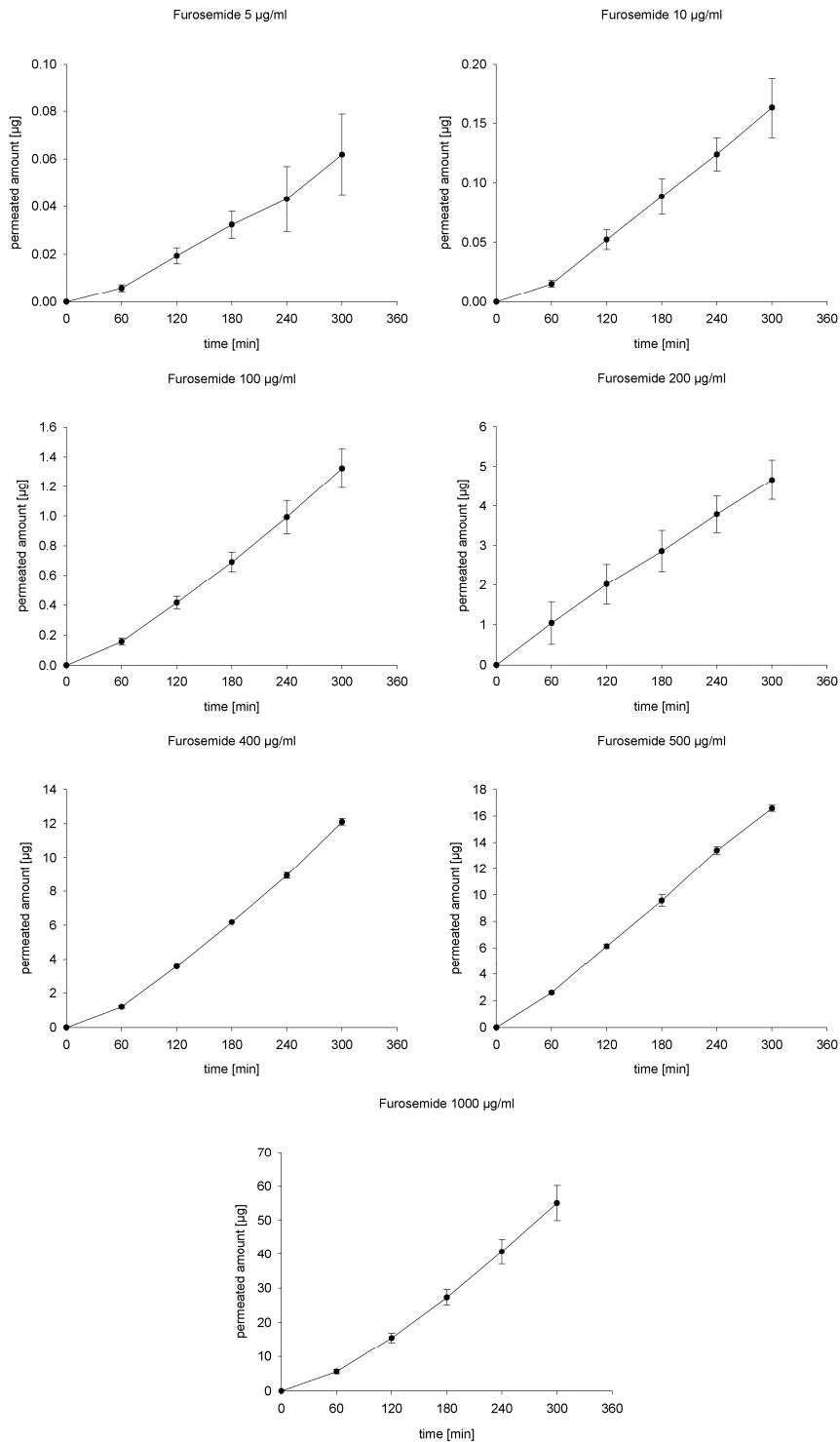


Figure 2-4 The graphs show the permeation of furosemide over Caco-2 cell monolayers at different donor concentrations in the Transwell® setup (n = 3).

Mean apparent permeability was calculated from the slope of the curves according to Equation 2-1 as $1.11 \pm 0.08 \times 10^{-6}$ cm/s, $1.75 \pm 0.02 \times 10^{-6}$ cm/s and $3.08 \pm 0.28 \times 10^{-6}$ cm/s.

$$P_{app} = \frac{dQ}{dt} \times \frac{1}{A \times c_d} \quad \text{Equation 2-1}$$

The experiments pointed out that the apparent permeability tended to rise with increasing donor concentrations. Next to the already mentioned asymmetrical transport of furosemide across Caco-2 monolayers this finding further supported the assumption that furosemide is subject to apical efflux transport. The status of saturation of an efflux transporter is supposed to be dependent on the donor concentration which influences the apparent permeability coefficient. So, a decreasing influence of the efflux transport with increasing substrate concentration can be expected, which is very similar to a Michaelis-Menten kinetic.

c Donor [$\mu\text{g/ml}$]	P_{app} [cm/s]
5	$0.67 \pm 0.20 \times 10^{-6}$
10	$0.84 \pm 0.01 \times 10^{-6}$
100	$0.72 \pm 0.08 \times 10^{-6}$
200	$1.11 \pm 0.08 \times 10^{-6}$
400	$1.68 \pm 0.05 \times 10^{-6}$
500	$1.75 \pm 0.02 \times 10^{-6}$
1000	$3.08 \pm 0.28 \times 10^{-6}$

Table 2-1 Apparent permeability coefficients (P_{app}) calculated from the linear part of the permeation curves shown in Figure 2-4.

After analyzing additional donor concentrations of 5 $\mu\text{g/ml}$, 10 $\mu\text{g/ml}$, 100 $\mu\text{g/ml}$ and 400 $\mu\text{g/ml}$ (Figure 2-4), the assumption of a dependency

between donor concentration and apparent permeability was confirmed (Figure 2-5). An overview of the calculated Papp values can be found in (Table 2-1). Within the range of concentrations that were analyzed, a linear ($R^2 = 0.98$) concentration dependency was found supposing that the concentration for saturation for the efflux transport is considerably higher than 1000 $\mu\text{g/ml}$ (Figure 2-5).

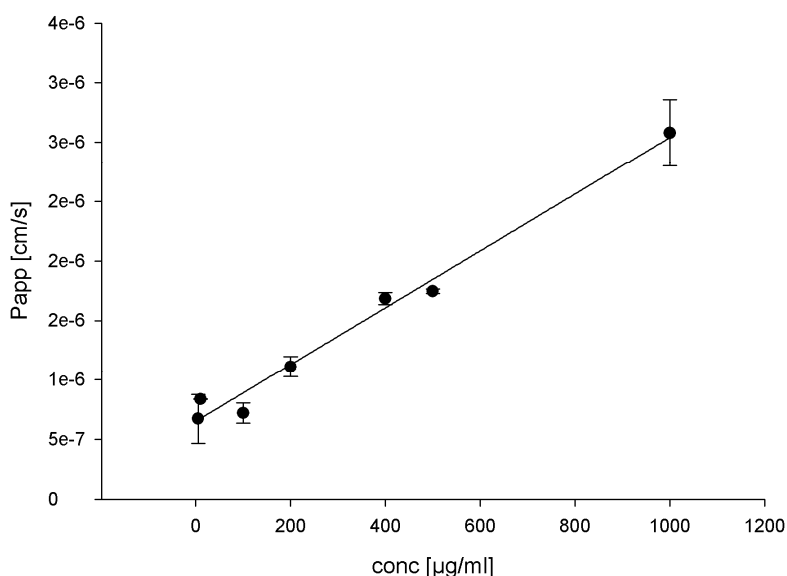


Figure 2-5 Dependency of the apparent permeability from the furosemide donor concentration.

But as this topic was not the most urgent matter of research, no further experiments were done here. Visualizing these results it was concluded, that the absolute level of donor concentrations might have an influence on the overall extent of permeation and thereby the partial saturation of efflux transport may contribute to the unexpectedly high permeation of furosemide within the apparatus. On the other hand, it had to be considered that with $2.5 \times 10^{-5} \text{ cm/s}$ [62] the apparent permeability of propranolol was still approximately ten times higher as that obtained for the highest donor concentration of furosemide. Furthermore, analyzing

tablets in the apparatus, high donor concentrations are effective only for the time when the peak concentration of the released compound is reached. In conclusion it is unlikely that the partial saturation of efflux transport by high donor concentrations of furosemide was the major reason for its unexpectedly high permeation.

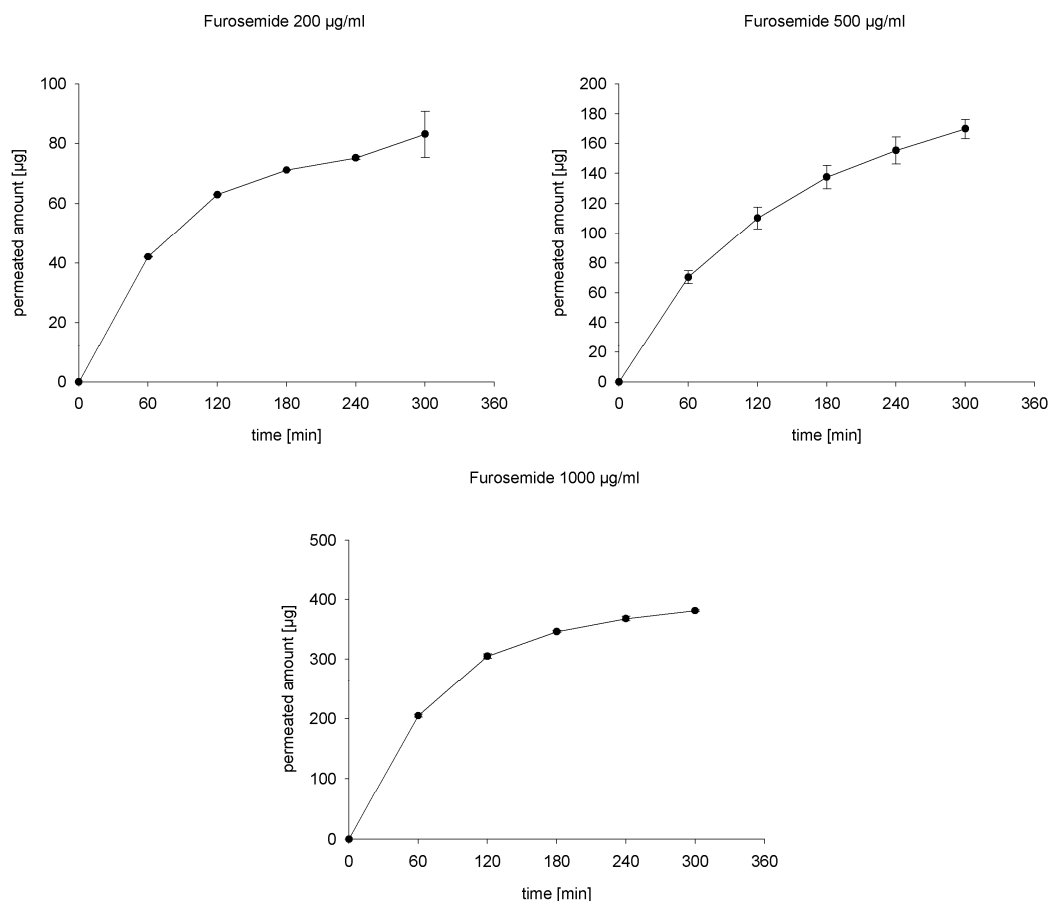


Figure 2-6 Permeation of furosemide over blank Transwell[®] supports at three different donor concentrations (n = 3).

As a control, experiments with blank Transwell[®] supports were conducted, clearly demonstrating that the filter membrane does not pose a significant hindrance for drug permeation (Figure 2-6). A non linear behaviour was obtained due to a quick depletion of the donor concentration leading to non sink conditions.

2.2.3 Permeation in the apparatus

The performance of Lasix[®] 40 mg IR tablets in the apparatus was evaluated in three experiments. The graph supposed a rapid accumulation of the drug in the basolateral compartment with a following depletion over time which was unexpected, as the apparatus featured a closed basolateral compartment (Figure 2-7).

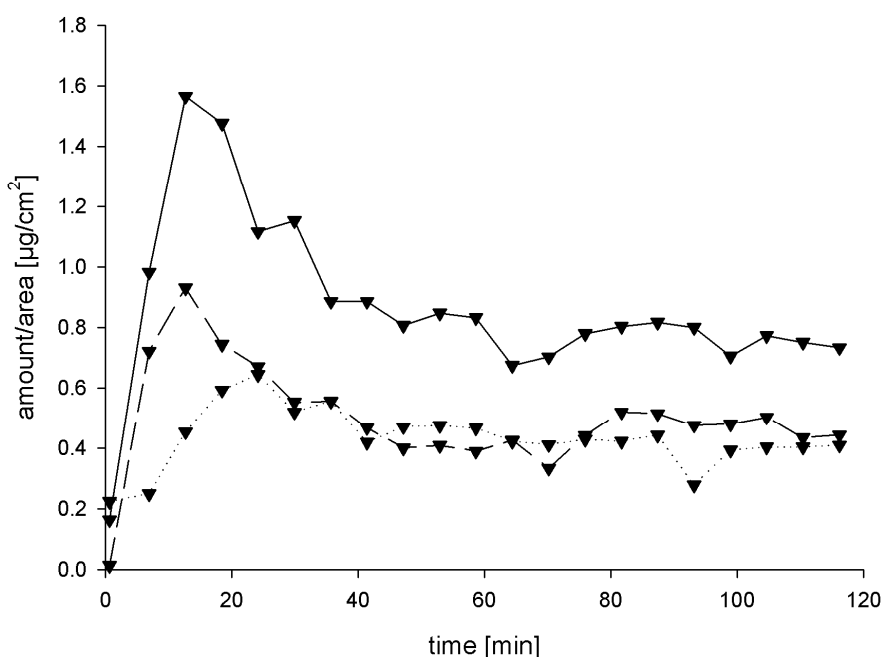


Figure 2-7 Basolaterally measured amount of furosemide after dissolution of Lasix[®] tablets at the donor side.

A back diffusion of the drug as a potential reason for the depletion of furosemide from the basolateral compartment was regarded as highly unlikely, as the absolute concentrations measured at the apical side were consistently higher as those measured in the basolateral compartment throughout the whole time of the experiments. Drug release from the Lasix[®] tablet was incomplete applying a membrane dosage pump with a

pulsation absorber as dissolution pump. Under those conditions providing a laminar flow inside the dissolution cell the compound was not dissolved completely which might be primarily addressed to the fact that the compound shows severe wetting issues next to the fact that the Lasix[®] formulation lacks in a modern “superdisintegrant” as e.g. cross-linked polyvinylpyrrolidone or cross-linked sodium carboxymethylcellulose (Figure 2-8).

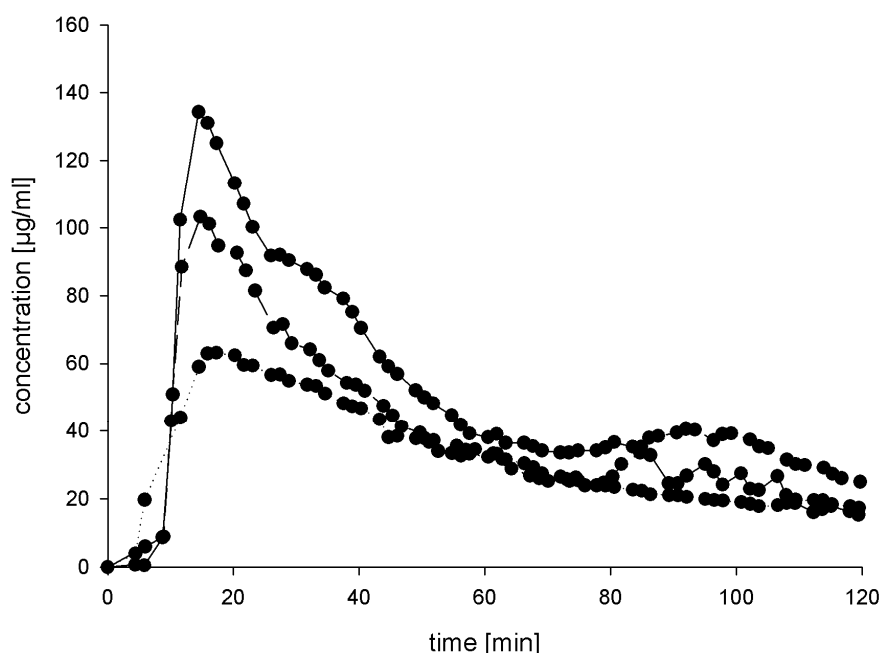


Figure 2-8 Apical concentrations analyzing Lasix[®] tablets with the apparatus as pointed out in Figure 2-1 (n = 3).

In order to reduce the number of variables and allow better comparability to the situation in the Transwell[®] setup, furosemide donor solutions providing a constant concentration on the apical side were analyzed instead of the tablets. Similar to the results that were obtained with the tablets high initial amounts of drug were detected at the basolateral port

(Figure 2-9). For the rest of the time the drug amount increased slightly but this did not happen in a linear way as would have been expected.

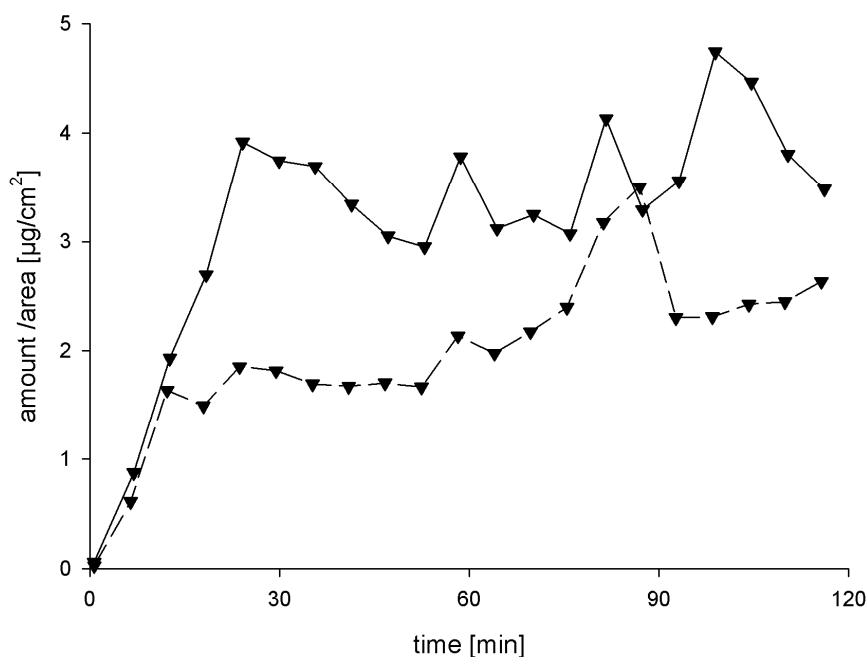


Figure 2-9 Amounts of furosemide measured at the basolateral side after application of donor solutions ($c = 200 \mu\text{g/ml}$) did not show a linear trend ($n = 2$).

Sorption of the compound to an internal surface of the basolateral circulation was considered as a potential reason that might explain the undulating behaviour of the basolaterally measured amount of drug. Polyetheretherketon (PEEK), the material that e.g. the basolateral vessel consists of, was excluded as a potential originator (data not shown). The remaining critical surfaces like peristaltic pump tubing and the interior of the pulsation absorbers were more difficult to analyze. In comprehensive experiments, furosemide solutions were pumped within the basolateral circulation and samples that were taken manually from the basolateral vessel revealed undulating concentrations within this compartment. Although these experiments could not definitely clarify if the

inhomogeneous concentrations found in the basolateral compartment had to be attributed to sorption issues or insufficient mixing the finding led the focus for troubleshooting on the basolateral compartment.

2.2.3.1 Simplified basolateral conditions

Furosemide permeation was measured in a simplified basolateral surrounding, as it was suspected that the non linear permeation behaviour of furosemide in the FTPC might be attributed to the basolateral compartment. Waiving the complete basolateral circulation, the setup was put into an apically dynamic and basolaterally static situation.

Experiment No.	TEER before experiment [$\Omega \times \text{cm}^2$]	TEER after experiment [$\Omega \times \text{cm}^2$]
1	477	310
2	504	407
3	449	468
4	477	534

Table 2-2 TEER of Caco-2 cell monolayers measured before and after conduction of experiments with simplified basolateral conditions.

Consequently, the basolateral vessel, the standard sampling point on the receiver side, was not hooked up and therefore the samples were drawn directly from the basolateral cavity of the FTPC using a syringe. These experiments were conducted without application of a counter-pressure from the basolateral side, as no pump was installed. Caco-2 cells were checked microscopically and proofed to be intact before and after the experiments which was also confirmed by TEER measurements (Table 2-2). In this setup, that circumvented the basolateral circulation and limited the volume of the acceptor compartment to the space inside the basolateral cavity of the FTPC, furosemide permeated linearly across the

Caco-2 cell monolayers (Figure 2-10). Therefore, the strange permeation behaviour that was found before was attributed to the basolateral circulation and consequently it was decided that the basolateral compartment should be revised.

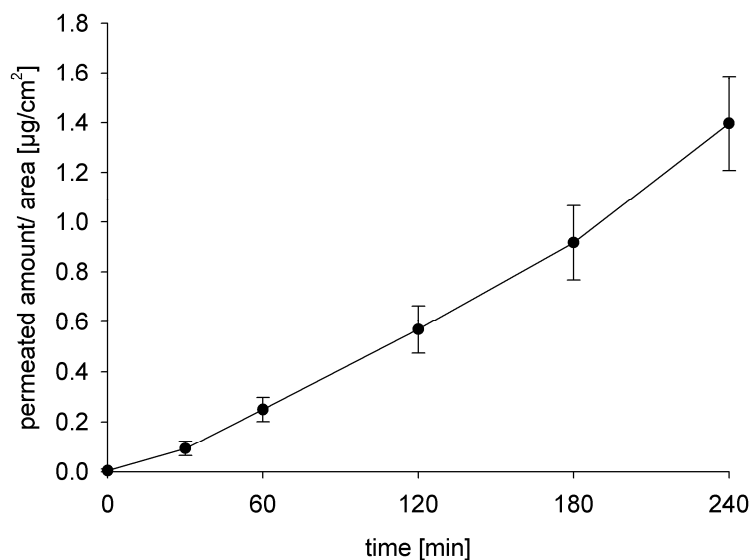


Figure 2-10 Permeation of furosemide in the FTPC under simplified basolateral conditions. P_{app} was calculated to $0.47 \pm 0.10 \times 10^{-6}$ cm/s for $n = 4$ experiments.

2.3 Revision of the basolateral compartment

The original basolateral compartment featured a transfer cycle driven by a membrane dosage pump and a measurement cycle driven by a peristaltic pump (Figure 2-11). One drawback was seen in the multiple subdivisions of the compartment rising questions about the homogeneous distribution of the accumulating drug inside the acceptor buffer. Secondly, the usage of peristaltic tubing was considered as critical, due to potential sorption and migration issues of lipophilic compounds.

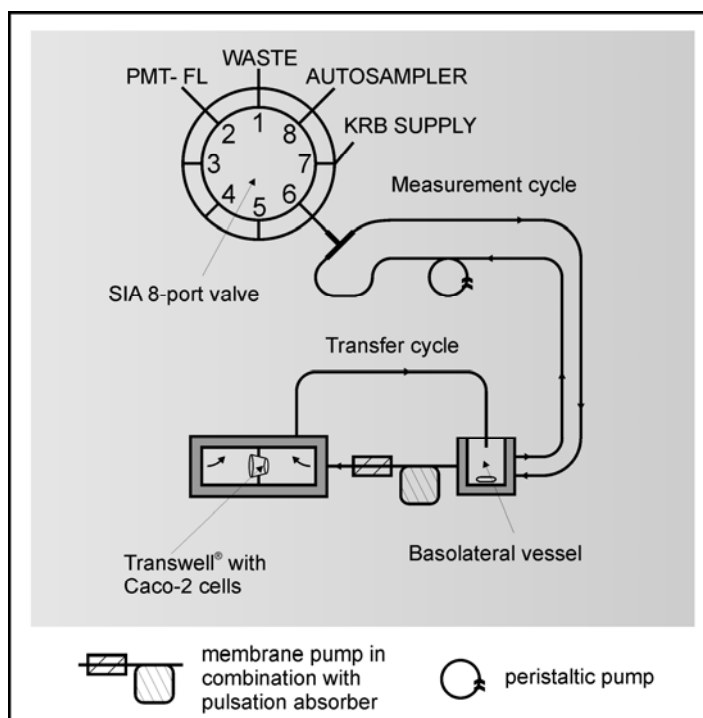


Figure 2-11 The original basolateral compartment featuring a transfer cycle driven by a membrane dosage pump and a measurement cycle driven by a peristaltic pump.

Due to the promising results that were obtained with the FTPC using a basolaterally static compartment, this approach was taken as a starting point for the reconstruction of the basolateral compartment. So, it was regarded as favourable to limit the compartment to the space of the

basolateral cavity of the FTPC itself. As this scenario no longer featured a flow through environment, a magnetic stirrer was integrated to provide a homogeneous distribution of the drug in the acceptor buffer. Therefore, the space of the basolateral cavity had to be enlarged slightly. Nevertheless, a reduction of the overall volume of the basolateral compartment from formerly 5.5 to now 3.8 ml was yielded. The basolateral pump with pulsation absorber, the interconnecting peristaltic tubing and the basolateral vessel could be waived (Figure 2-12).

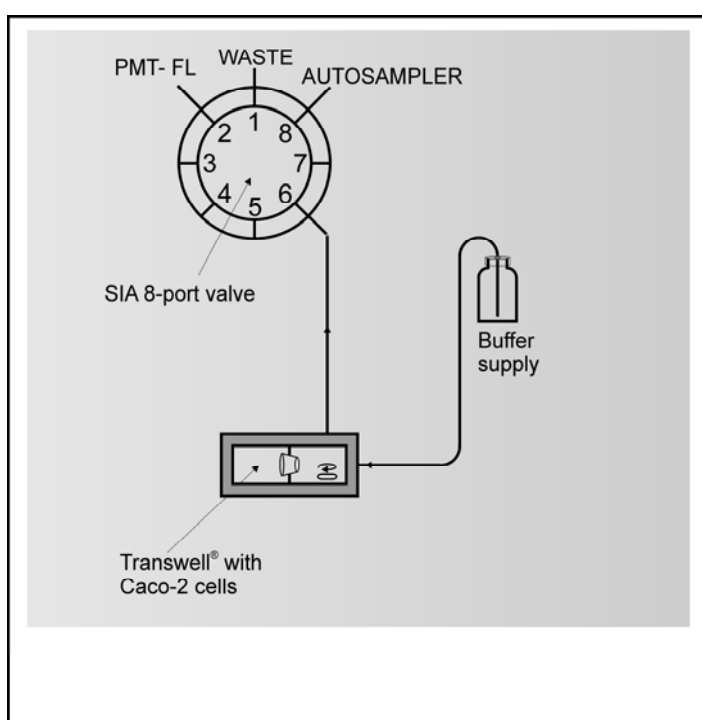


Figure 2-12 Schematic depiction of the revised basolateral compartment, limiting the acceptor volume to the space of the basolateral cavity of the FTPC.

A detail drawing of the FTPC after revision can be seen in Figure 3-1. By means of these adaptations the above-mentioned questions could be dispelled and in addition a simplification of the handling was reached.

2.4 Hydrostatic pressure compensation between apical and basolateral side of the FTPC

Caco-2 cells grown on permeable supports are sensitive to pressure differences between the two compartments. Especially pressure from the basolateral side has to be avoided, as this may lead to a detachment of the cells from the supporting membrane. In the original setup equal pressure weighing on both sides of the cell monolayer was warranted by symmetrical installation of two membrane dosage pumps providing equal flow rates through the apical and the basolateral cavity of the FTPC.

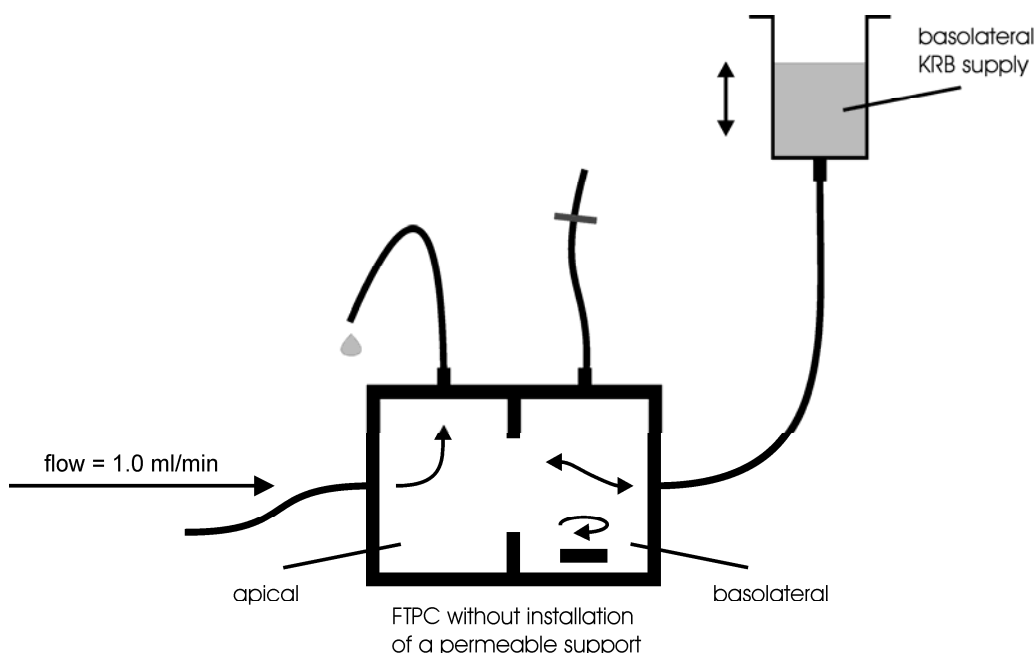


Figure 2-13 The necessary basolateral counter pressure to the apical flow can be determined without installation of a Transwell[®] inside the FTPC. The liquid column at the basolateral KRB supply will adjust to a height that provides a corresponding hydrostatic counter pressure to the apical flow. After equilibration the height of the suitable liquid column can be read out and will provide apical to basolateral pressure balance in experiments with a Caco-2 cell monolayer mounted between the compartments. In this setup replenishment of the sample volumes with blank KRB is provided automatically.

In the revised setup the basolateral pump was waived and pressure balance was reached applying a suitable hydrostatic counter-pressure from the basolateral side (Figure 2-13). Therefore, the tube of a 100 ml syringe was filled with KRB, fixed inside the water bath and connected with the FTPC by means of polymeric tubing.

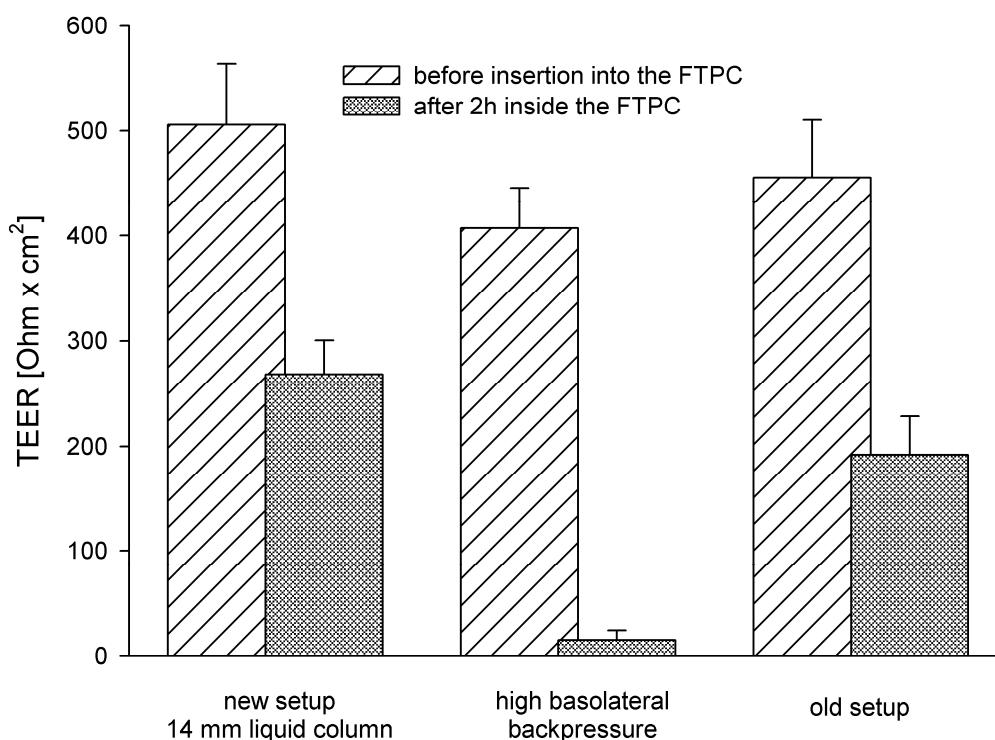


Figure 2-14 TEER of Caco-2 cell monolayers before insertion into and after 2 hours inside the FTPC.

To determine the necessary counter pressure, the FTPC was assembled without insertion of a Transwell®, the internal space was prefilled with KRB and the apical pump was switched on. The meniscus of the liquid column inside the basolateral KRB supply, was read after equilibration of the system as 14.0 ml above the bottom level of the FTPC. This level was adjusted in experiments comprising Caco-2 cells. TEER measurement before and after the experiments revealed that this procedure provided a

suitable pressure compensation which was not inferior to the method applied in the original setup (Figure 2-14).

2.5 Influence of automated sampling on permeation results

After revision of the basolateral compartment the application of a donor concentration of 200 µg/ml resulted in a lower linearity of the permeation as obtained in the preceding experiments with the reduced basolateral compartment and manual sampling (Figure 2-15).

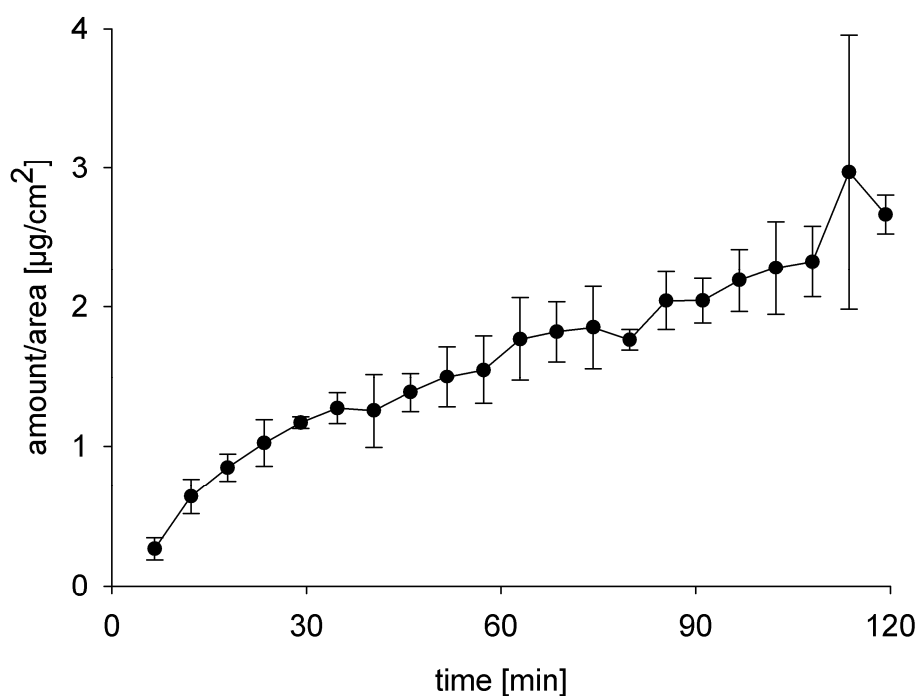


Figure 2-15 Basolateral permeation of furosemide after application of 200 µg/ml donor solutions with the new basolateral compartment (n = 3).

Nevertheless the calculated P_{app} of $1.34 \pm 0.10 \times 10^{-6}$ cm/s corresponded to the results that were obtained in the Transwell[®] setup (Table 2-1). After

studying the donor solutions the performance of the apparatus using Lasix[®] tablets was evaluated revealing that the results were still not as expected (Figure 2-16). Especially the decreasing amount of furosemide measured at sampling point B cannot be explained as the setup after revision is still built up as a closed compartment and therefore an accumulation of the drug was expected.

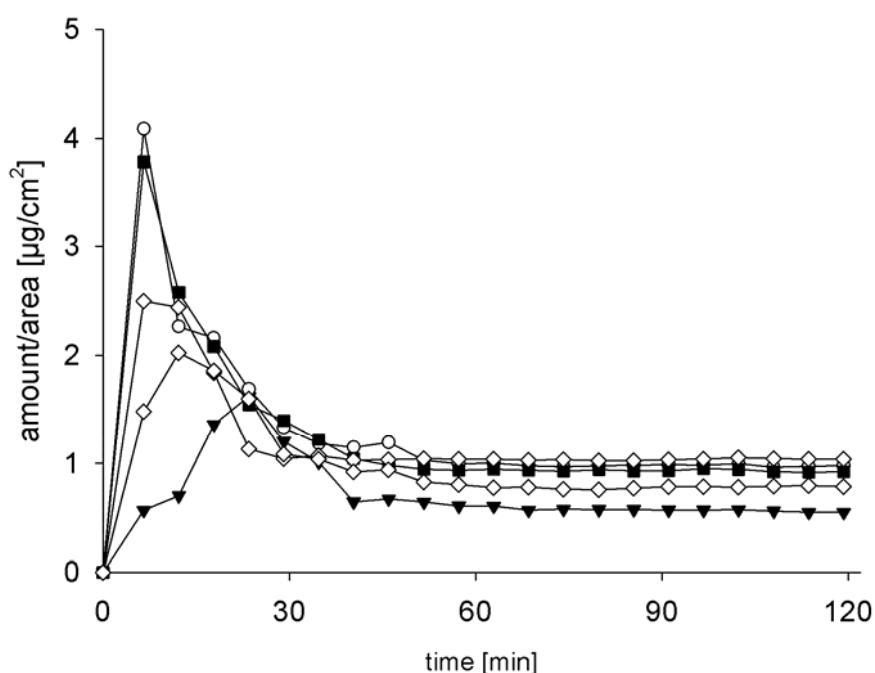


Figure 2-16 Basolateral amount of furosemide after analysis of Lasix[®] 40 mg IR tablets (n = 5).

So, further efforts to solve these questions had to be taken. In order to clarify if the drug measured at point B really took the way across the Caco-2 cell monolayer an impermeable Transwell[®] with pores that were sealed with varnish was used in the successive experiments. To simplify the detection in the following experiments propranolol donor solutions instead of furosemide solutions were used as in this case online detection was feasible at all three measurement points, whereas analysis of the

basolateral samples of furosemide required HPLC analysis. This was possible as the question that should be addressed was not depending on the nature of the compound. Using a 60 µg/ml propranolol donor solution a basolateral signal was observed, although the connection between the donor and the acceptor compartment was sealed (Figure 2-17).

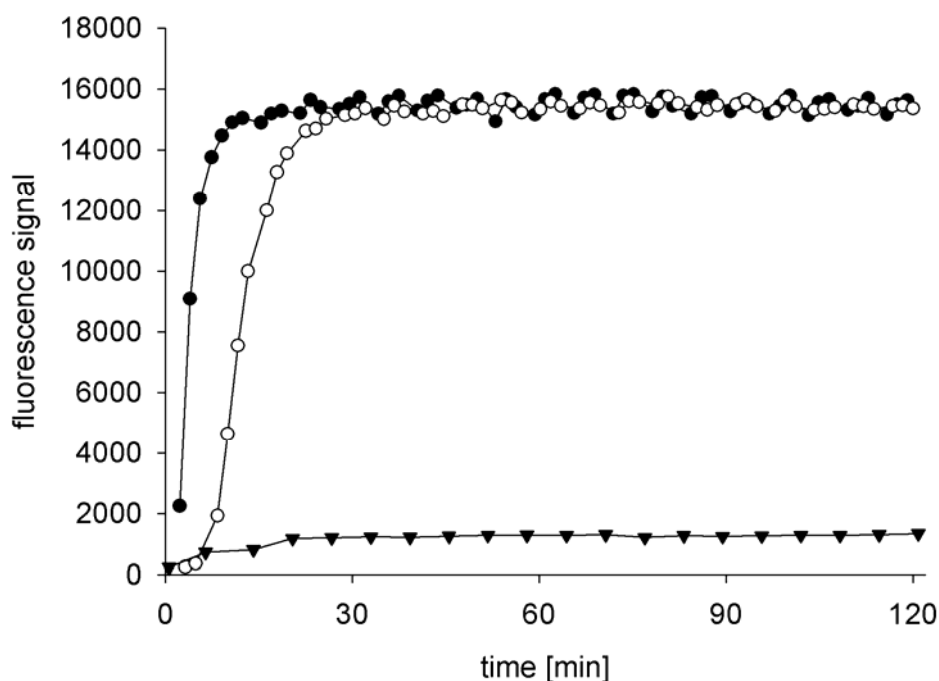


Figure 2-17 Fluorescence signals measured in the revised setup at sampling port D (●), A (○) and B (▼) using an impermeable Transwell® support and a propranolol donor solution.

After this important finding two more possibilities were conceivable. Either there was a leakage between the impermeable Transwell® and the O-ring inside the FTPC or the basolateral signal dated from a separation issue at the multiposition valve. This question could be clarified in a second experiment plunging the tubing for aspiration of basolateral samples into a vessel containing blank KRB. In this experiment an identical result as in the first one was obtained (Figure 2-18) which allowed the conclusion that

the conflicting results can only be ascribed to a problem at the multiposition valve.

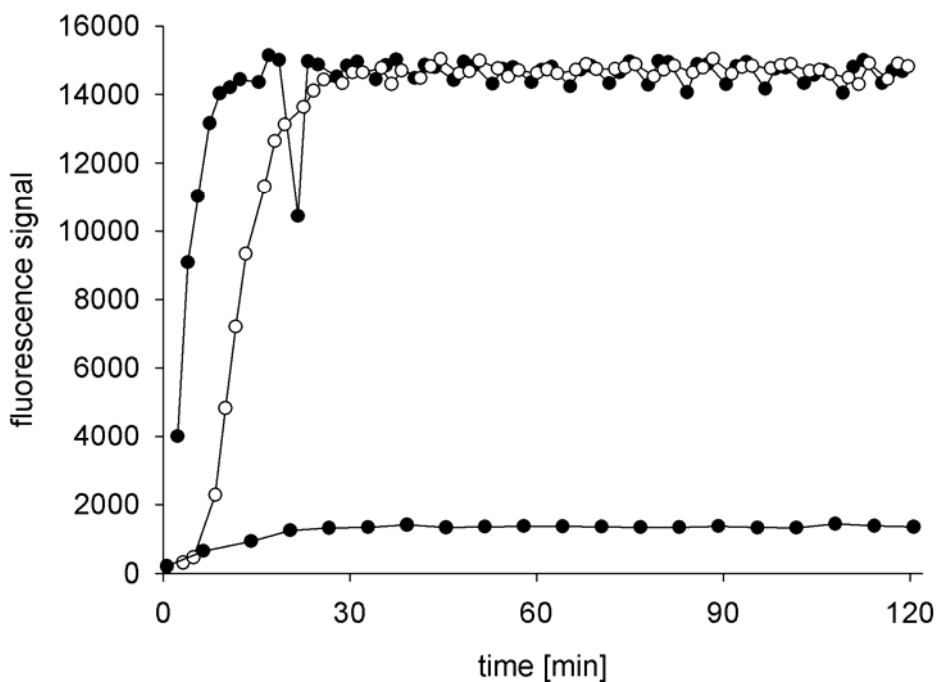


Figure 2-18 Fluorescence signals measured in the revised setup at sampling ports D (●) and A (○) applying a 60 µg/ml donor solution and aspirating blank buffer at measurement point B (▼).

2.6 Test routine for SIA valves

The findings of the experiments using an impermeable Transwell® indicated that the problem was located at the multiposition valve. In order to quantify the carry-over between the individual ports of the 8 port SIA valve a test routine was developed and a simple experiment using two sampling ports, one blank and one propranolol solution was performed. The SIA was programmed to sample alternately at two neighbouring ports. When both ports took their samples out of the blank, no fluorescence

signal was detected. When one of the ports took its sample out of the vessel containing the drug solution and the other still out of the blank, there was a signal detectable at the port that only aspirated blank buffer (Figure 2-19).

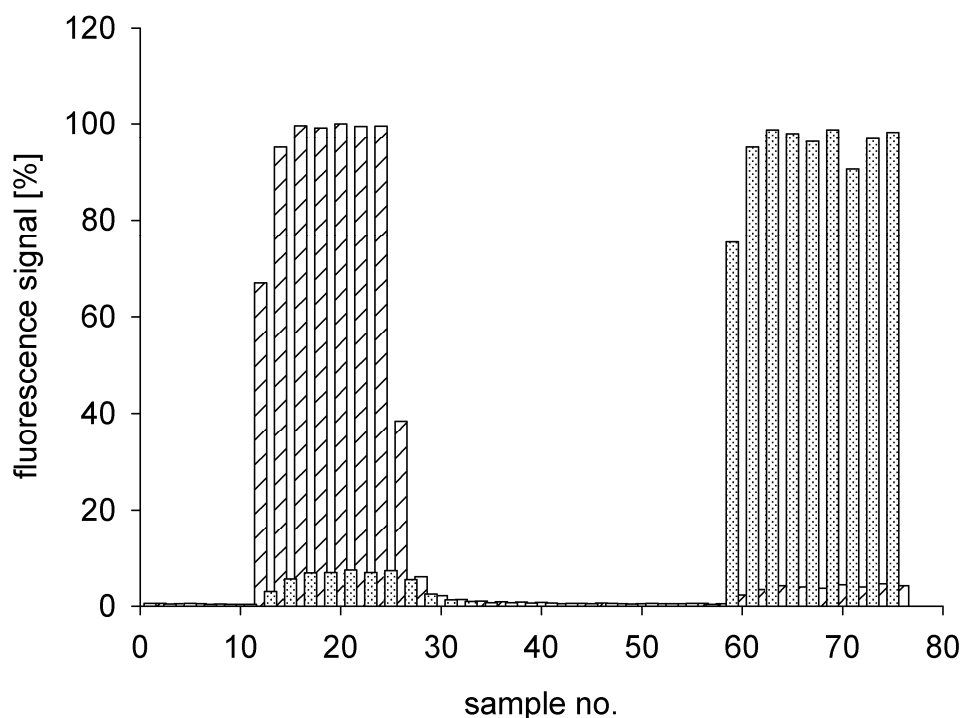


Figure 2-19 Fluorescence signals obtained during alternating sampling at 2 neighbouring ports. During the times that now signal was retrieved both ports took their samples from a blank solution. Signals were detectable at both ports, when one port was sampling blank buffer and the other port a propranolol solution.

This proved that the multiposition valve was not able to separate samples from different ports completely. After consultation of the SIA manufacturer (FIALab instruments, Sarrasota, FL) on those results it was decided to renew the 8 port valve in order to warrant the optimum performance of the setup. After mounting of the replacement valve the experiment was repeated and a better, but still incomplete separation was obtained.

Further experiments pointed out that the intrinsic carry-over of the valve lies between 0.5 and 1% (Figure 2-20).

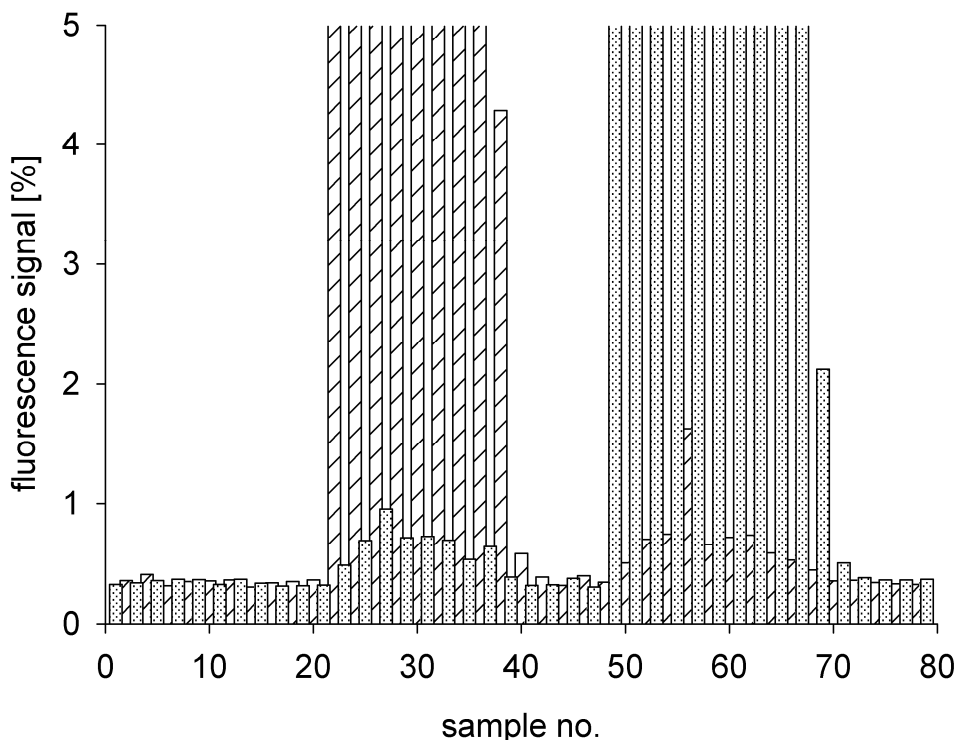


Figure 2-20 Determination of the carry-over between 2 neighbouring ports after installation of a new 8 port multi position valve.

This bias is tolerable for the analysis of high permeable compounds, like propranolol. Here, a drug concentration of approximately 5% of a constant donor solution after two hours can be expected (Figure 2-21). That means that the bias of the carry-over effect is surmounted already 20 minutes after start of the experiment and therefore it was regarded as negligible. For the analysis of low permeable compounds the situation is different. Due to the low flux over Caco-2 monolayers the basolateral concentration increases slowly. Calculating the basolateral concentrations of a compound with a P_{app} of 5×10^{-7} cm/s after two hours with a constant

donor concentration and an acceptor volume of 3.8 ml a value of less than 1% of the donor concentration has to be expected. That means that in this case the bias of the carry-over effect does not allow measuring the permeation rate of such a compound simultaneously to the concentration at the donor side.

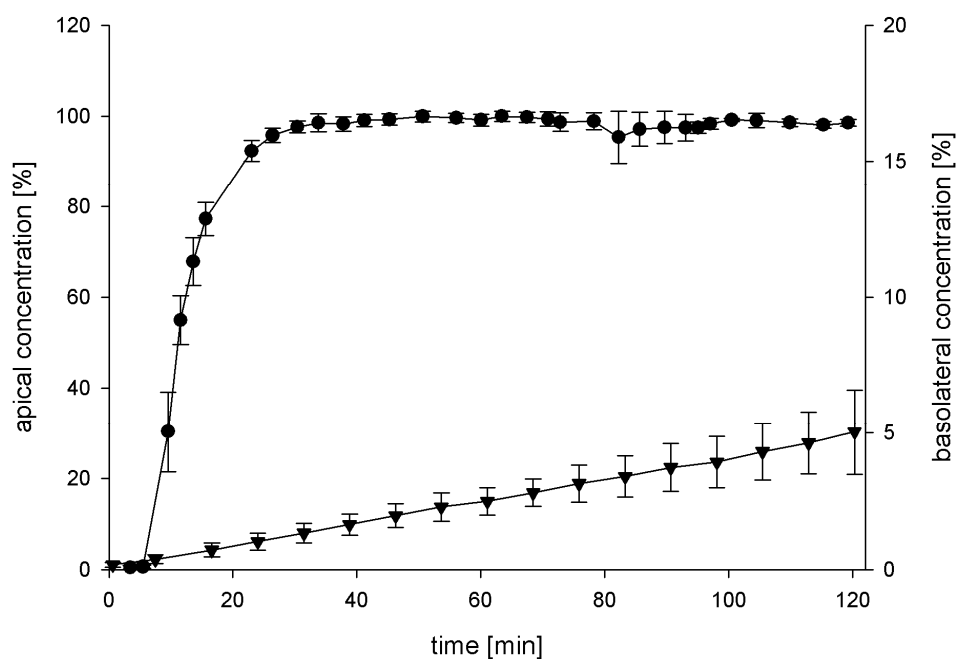


Figure 2-21 Concentration time trend of propranolol donor solutions ($c = 20 \mu\text{g/ml}$) at the apical and the basolateral sampling point ($n = 3$).

2.7 Implementation of an independent route for basolateral sampling

Simultaneous sampling of high concentrations at ports D and A next to the analysis of low concentrations at port B using only one multiposition valve turned out to be impossible due to an intrinsic carry-over biasing the results for the low concentrations.

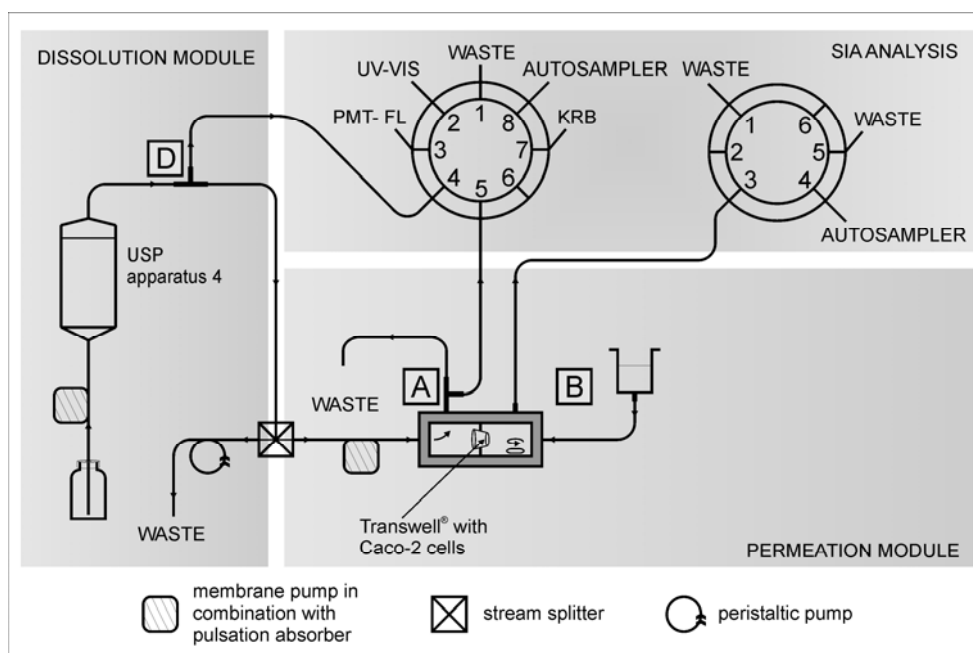


Figure 2-22 The figure shows a schematic overview of the revised apparatus featuring the dissolution module, the permeation module and a third module for automation using Sequential Injection Analysis (SIA). Dissolution takes place in a compendial flow through cell (Apparatus 4 USP). Samples of the high concentrations right behind the dissolution cell and at the outflow of the apical compartment are taken via an 8 port multiposition valve and analyzed online using an UV-VIS spectrometer or a fluorescence detector (PMT-FL). Samples of the acceptor compartment are taken via an additional 6 port valve and analysis is done offline in a plate reader or by means of HPLC measurement after bottling with an autosampler.

As it turned out to be technically impossible to circumvent that carry-over effect with the existing equipment it was decided to install a separate route

of sampling for the basolateral compartment. Therefore, a second syringe pump, a 6 port valve and an autosampler were installed. A schematic overview of the automated setup can be seen in Figure 2-22.

2.8 Performance test of the revised apparatus

After revision of the basolateral compartment and installation of an independent route for basolateral sampling the setup was tested with the marker compounds sodium fluorescein and rhodamine 123 using fluorescence detection ($\lambda_{\text{ex}} = 485 \text{ nm}$, $\lambda_{\text{em}} = 530 \text{ nm}$).

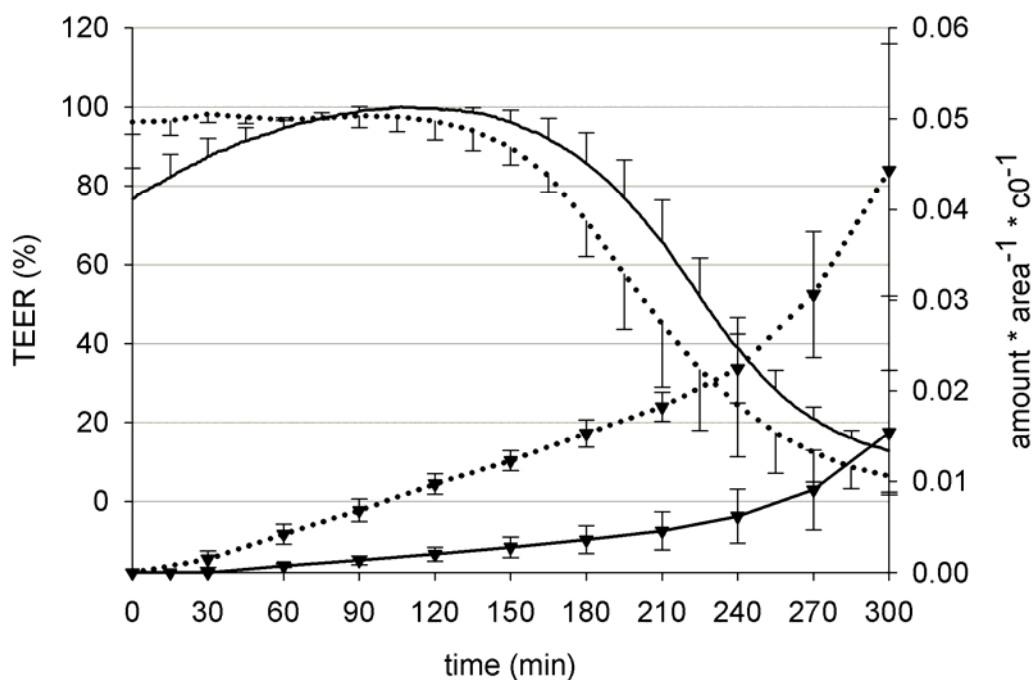


Figure 2-23 Permeation of sodium fluorescein (▼ continuous line) and rhodamine 123 (▼ dotted line) in the revised setup after installation of an independent route for basolateral sampling using donor solutions. Simultaneously to the permeation transepithelial electrical resistance (TEER) was recorded in the FTPC as a measure for the status of the paracellular barrier of the Caco-2 cells (see chapter 3).

After application of constant donor concentrations on the apical side, a linear permeation for 3.5 hours was observed for both compounds (Figure 2-23). P_{app} was calculated to 1.4×10^{-6} cm/s for rhodamine 123 and to 4.0×10^{-7} cm/s for sodium fluorescein. Troutman and Thakker reported a permeability of 1.5×10^{-6} cm/s [70] for rhodamine 123 and for sodium fluorescein P_{app} values ranging from $2.1 - 6.23 \times 10^{-7}$ cm/s have been reported [71-74]. So, the permeability of the marker compounds is in good agreement to the values reported in the literature pointing out the suitability of the revised setup for the analysis of low permeable compounds. When these experiments were conducted the FTPC was already implemented with electrodes for measurement of TEER which therefore was recorded simultaneously to the permeation assessment (Figure 2-23). TEER remained on a high level for approximately 3.5 hours pointing out the time span of cell monolayer integrity. Only when TEER dropped to low values, permeation rate of sodium fluorescein and rhodamine 123 increased strongly. The remaining question about the analysis of furosemide oral formulations is discussed in chapter 4.

3 Online TEER measurement

Parts of this section have been published in:

Muendoerfer, M., et al., Online monitoring of transepithelial electrical resistance (TEER) in an apparatus for combined dissolution and permeation testing. *Int J Pharm*, 2010. 392(1-2): p. 134-40.

3.1 Rational for the implementation of online TEER measurement

Two major benefits were aimed for by means of developing a feature for online TEER measurement inside the apparatus for combined measurement of dissolution and permeation. First of all there was an urgent need for a tool that provided feedback on the status of the cell monolayer inside the FTPC during the course of an experiment. Prior to that, it was only possible to analyze a cell monolayer before and after an experiment outside the FTPC. This was considered as insufficient as e.g. handling of the cells and change of buffer solutions causes temperature drops which are well known to influence TEER [75]. Therefore, online TEER measurement should serve as a tool for surveillance of the cell monolayer and was supposed to be a means for in-line control supporting the results of each experiment. In addition to that the novel feature should be tested for its suitability as a tool to analyze the effects of excipients on cell monolayer permeability. In this context it was supposed that online TEER measurement might be a valuable improvement of the apparatus regarding its scope as a tool for the advanced formulation screening of BCS class III or IV compounds.

3.2 Introduction into TEER measurement

3.2.1 TEER and tight junctions

Measurement of TEER is a well established method for the non-destructive and non-invasive monitoring of the barrier status of cellular layers grown on permeable supports. As long as in this case the Caco-2 cells have not reached confluence TEER stays at a low level, close to the blank resistance of the permeable support. Only after the epithelial cells reach confluence they stop proliferation and start to differentiate. This gets visible in a polarization of the cells into an apical and a basolateral side. Next to that it comes to the formation of the so called tight junctions between neighbouring cells [39]. These protein based structures surround the lateral sides of the cells in the upper third, close to the apical end in a belt-like shape. Completely developed, the tight junctions seal the cellular interspaces and provide the rate limiting barrier for the passive paracellular transport of solutes [76, 77]. The mesh-like structure formed by individual protein strands can be visualized in freeze fracture replicas [78]. This method also allows pointing out the fence function of the tight junctions. After application from the basolateral side, macromolecules as horseradish peroxidase or haemoglobin diffuse freely along the paracellular interspaces until reaching the tight junctional strands [79]. Electrophysiological characterization of epithelial cell monolayers revealed junctional charge and size-selectivity and allowed the determination of the pores, formed by the tight junctions to be mainly permeable to sodium ions [80]. According to the latest findings on the molecular assembly of the tight junctions these structures are composed by protein clusters of the Claudine family [81, 82]. These proteins feature two extracellular domains carrying either negative or positive excess charges according to the individual distribution of acidic or basic amino acids. In a potential spatial model these protein aggregates are supposed to build pores with charged internal linings

conveying the well known charge and size restriction for paracellular solute transport.

3.2.2 Practical approaches for TEER measurement

TEER measurement is usually performed as single point measurement at certain points of time for example during the period of cellular growth in order to monitor the maturation of the cells of interest. In this case the measurement has to be conducted under sterile conditions inside a laminar flow box. During cellular growth the confluence of the cells to a monolayer is pointed out by an increase in TEER and the magnitude of TEER correlates with the tightness and impermeability of the cellular layer. The absolute level of TEER that a cell monolayer can reach is a cell type characteristic feature. The Caco-2 C2BBE1 clone in our lab typically reaches a value of $> 400 \Omega \times \text{cm}^2$ as soon as the cells have been passaged for the first few times after thawing. Nevertheless a broad range of TEER values for Caco-2 cells can be found in the literature spanning from 80 up to $1420 \Omega \times \text{cm}^2$ [83]. Reasons for this high variability may be found in different subclones, passage numbers and cultivation protocols of the cells.

TEER measurement can be performed in different ways:

1) Measurement with hand-held electrodes

The standard in cell culture associated TEER measurement is the single point measurement of TEER after insertion of a so called “chop-stick” electrode, (e.g. STX-2 electrode, World Precision Instruments, Sarasota, FL, USA) into the apical and the basolateral part of a multi-well culture plate with a cellular layer grown on top of a permeable support (e. g.,

Transwell[®], Corning Inc., NY, USA). Chopstick electrodes feature specially designed shanks so that after insertion into the well plate a direct contact between the apical electrode and the cellular layer is prevented. The readout of the resistance might for example be done with an EVOM2 (WPI, Sarasota, FL, USA) or the Millicell ERS-2 Epithelial Volt-Ohm Meter (Millipore, Billerica, MA, USA).

2) Measurement in Endohm chambers

Next to the use of hand-held electrodes it is also common to check TEER of a cell monolayer with a fixed set of electrodes inside a so called Endohm chamber (WPI) into which the permeable support has to be transferred into right before the measurement. This option features the advantage of a lower background resistance due to the optimized position of the electrodes and it also reduces the variability of the resistance readings. A disadvantage of this method is the necessity to transfer the permeable support from the experimental environment into the Endohm chamber and the need to replenish the apical and basolateral liquid volumes which is known to influence the absolute value of TEER [75].

3) Automated measurement of TEER in well plates

Furthermore, it is possible to measure TEER of monolayers grown on individual permeable supports inside one bottom plate in an automated way. Therefore, the well plate containing the permeable supports has to be handed over to an autosampler featuring an electrode fixed with a robotic arm, which allows sequential measurement of TEER of individual monolayers in combination with a computer control unit (REMS system; WPI).

4) Measurement of electrical resistance in non-cell based assays

Apart from cell culture associated TEER measurement it is also common to measure the electrical resistance of artificial membranes incorporated into well plates and intended for the high-throughput permeability screening of solutes after conduction of the respective experiment in order to check the integrity of the artificial membrane. This can for example be performed with the EVOM2, a hand held top electrode and WPI's Multi-96 bottom plate containing basolateral electrodes.

5) TEER measurement during cultivation of cell monolayers on permeable supports

A device for the measurement of transepithelial impedance and TEER of cell layers grown on permeable supports throughout the period of growth is commercially available ("cellZscope", nanoAnalytics GmbH, Münster, Germany). This product consists of a cell module which is placed inside an incubator, an external controller unit and a software as user interface. Further information to this approach can be found by Wegener et al. [84].

3.3 Realisation of TEER measurement inside the FTPC

As a first step towards online TEER measurement electrodes had to be installed inside the apical and the basolateral brick of the FTPC. As voltage sensors sintered silver-silver chloride bare sensor electrodes (In vivo Metric, Healdsburg, CA, USA) were chosen and as current electrodes pure silver wire has been used which from the choice of electrode-materials corresponds to the commercially available handheld STX-2 electrode (WPI). In detail, drillings have been added to the apical and the

basolateral brick of the FTPC that allow for the necessary wiring and the seamless implementation of the electrodes into the inner surface of the FTPC (Figure 3-1). At the outside of the bricks screw ports with 1/4-28 threads for connection with flangeless fitting adapters, made of PEEK, the identical material as used for the FTPC itself, have been integrated. These adapters were custom made at BESTA-Technik für Chromatographie GmbH, 69259 Wilhelmsfeld, Germany (Figure 6-1). The adapters serve as spacers for plugging in the cables to the EVOMX and provide a proper sealing against intrusion of water from the surrounding water bath. In the heads of these adapters plugs with M5 screw threads that are connected to the internal wiring have been mounted. Inside the adapters the wiring is led through a piece of 1/16" polymeric tubing which is tightened by means of a flangeless ferrule at the moment that the adapter is screwed in. To prevent a leakage line between wire and polymeric tubing, the wire has been sealed inside the tubing by means of a drop of superglue. At the

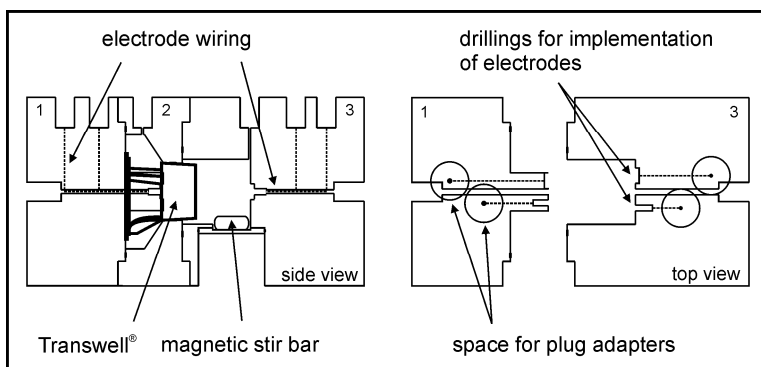


Figure 3-1 Detail drawing of the FTPC after revision of the basolateral compartment and implementation of electrodes for continuous TEER measurement.

basolateral brick the electrodes have been integrated into the backplane of the interior cavity. At the apical brick it turned out to be superior to mount the electrodes into the front tip instead of the backplane of the body, as hereby a lower background resistance and a better stability of the signal could be retrieved. This can be explained by the fact that this configuration

features a smaller distance between the electrodes and a more symmetric adjustment with regard to the cell monolayer. In this configuration the stream-lines of the electrical field are crossing the cell monolayer in rectangular direction without disturbance of any material of the PEEK housing (Figure 3-1).

3.4 Proof of principle using analogue recording

After hooking up the electrodes and connection of a writer (Kipp und Zonen, Germany) to the BNC output of the EVOMX, a continuous signal for TEER inside the FTPC could be recorded. In a first set of experiments the question in how far TEER values recorded outside and inside the FTPC are comparable was addressed. Therefore, TEER of three Caco-2 cell monolayers was measured by means of handheld electrodes before and after insertion into the FTPC in a Transwell[®] plate (Figure 3-2). In the interim time the monolayers were mounted inside the FTPC, the compartments were filled with KRB pH 7.4, an apical flow rate of 1.0 ml/min was applied and TEER was recorded (Figure 3-2). The experiments illustrated that after careful installation of a Transwell[®] a TEER similarly high as obtained directly before by manual measurement can be reached inside the FTPC. On the other hand a considerable difference between the TEER after two hours inside the FTPC and the manually obtained measurements after careful removal of the Transwell[®] supports from the FTPC was detected in all three experiments. These results suggested that the paracellular barrier function of the Caco-2 cells inside the FTPC might be kept for more than two hours and probably longer as suggested by TEER measurement outside the FTPC. A detailed analysis of this question can be found in chapter 3.6.

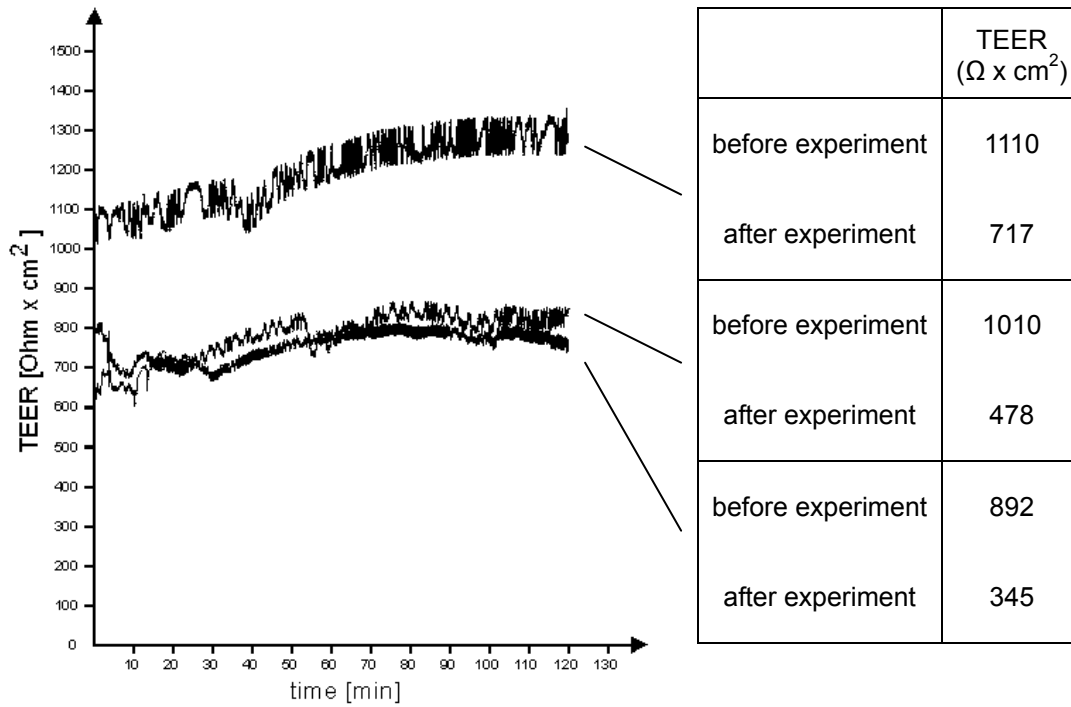


Figure 3-2 Left side: Online TEER profiles of three Caco-2 cell monolayers inside the FTPC. Right side: TEER of the identical monolayers measured inside a Transwell® plate before and after insertion into the FTPC.

3.5 Computer-controlled online TEER measurement

In a further step data acquisition was assigned to a computer after A/D conversion of the signal, and the EVOMX was customized with a digital input that allowed for software controlled triggering of the TEER measurement.

3.5.1 Adaption of the EVOMX

Concerning the measurement equipment it was decided to stay with the EVOMX which is optimized for cell culture conditions and uses a four point probe setup for voltage measurement. The device already features an analogue BNC output that allows tapping voltage readouts. In order to provide for an option to trigger the TEER measurement electronically the EVOMX was customized with a relay and an associated circuit. The resulting parallel connection of the closing switch now allowed both manual and electronic triggering of TEER measurement.

3.5.2 Computer-controlled measurement

In order to allow for the computer-controlled data acquisition and triggering of the measurement a multifunction data acquisition device (NI-USB 6009, National Instruments, Munich, Germany) in combination with LabVIEW software (Version 8.5, National Instruments, Munich, Germany) was used (Figure 3-3). A custom program called virtual instrument (VI) was developed providing a loop with adjustable parameters like measurement frequency, samples to average and delay-time before measuring. A sampling frequency of one per minute was chosen as default setting as it

proved to be sufficient to still speak of continuous TEER measurement and eliminated any potential questions regarding electrical polarization, electrode reactions or rapid material wearout.

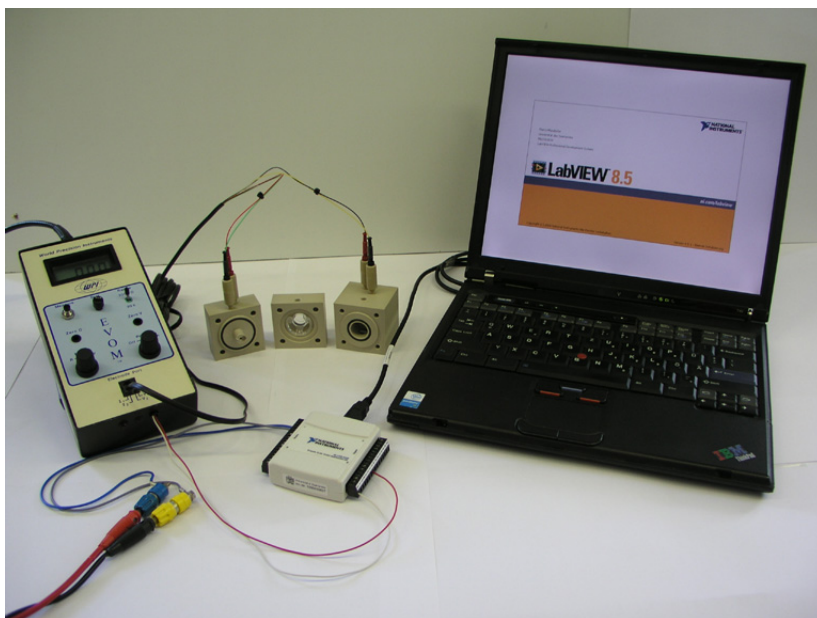


Figure 3-3 Overview of the components necessary for the computer controlled triggering and data acquisition of online TEER measurement inside the FTFC.

3.6 Lifetime of Caco-2 cells inside the FTFC

Aim of the study was to elucidate the time frame for which the Caco-2 cells keep up the paracellular barrier function. Therefore, two methods, online TEER and solute flux measurement were used concomitantly in order to monitor the status of the cell monolayer inside the FTFC. Sodium fluorescein was used as a hydrophilic marker compound for analysis of the paracellular permeability. Krebs Ringer Buffer (KRB) pH 7.4 was used as acceptor medium and as a basis for the donor solution containing a concentration of 5 $\mu\text{g/ml}$ sodium fluorescein in KRB pH 7.4 (Flu-KRB). In the present study no solid formulations were applied. Therefore, the

dissolution equipment remained out of operation and the buffer solutions were pumped through the apical compartment of the FTPC directly. For this purpose a Stepdos 03[®] membrane dosage pump in combination with a pulsation absorber (KNF Neuberger, Freiburg, Germany) was used. The flow rate of the pump was set to 1.0 ml/min. Before each experiment a Caco-2 monolayer grown on a Transwell[®] support was inserted into the FTPC, both compartments were filled with preheated KRB and the apical pump was switched on. After 15 minutes of equilibration the experiments were started by the activation of computer controlled TEER measurement and automated sampling. A switch of donor solutions was conducted equally in all experiments from blank KRB to Flu-KRB in order to check the tightness of the cell monolayer. This switch did not show any influence on the course of TEER. Figure 3-4 shows the permeation of sodium fluorescein and reveals that the Caco-2 cell monolayers keep up their barrier properties inside the FTPC for nearly 3.5 hours after the start of an experiment. The application of the constant donor concentration of 5 µg/ml sodium fluorescein at the apical side led to a linear permeation behaviour of the compound as long as TEER remained on a high level. A mean apparent permeability of $0.4 \pm 0.18 \times 10^{-6}$ cm/s was calculated from the slope of the linear part of the permeated amount between 60 and 180 minutes. This value lies within the range of reported Caco-2 permeability for sodium fluorescein of $0.21 - 0.623 \times 10^{-6}$ cm/s [73, 74] and permeability did not increase until TEER dropped below $300 \Omega \times \text{cm}^2$. When the time of cell monolayer integrity had expired, TEER dropped to low values and at the same time the permeability increased strongly.

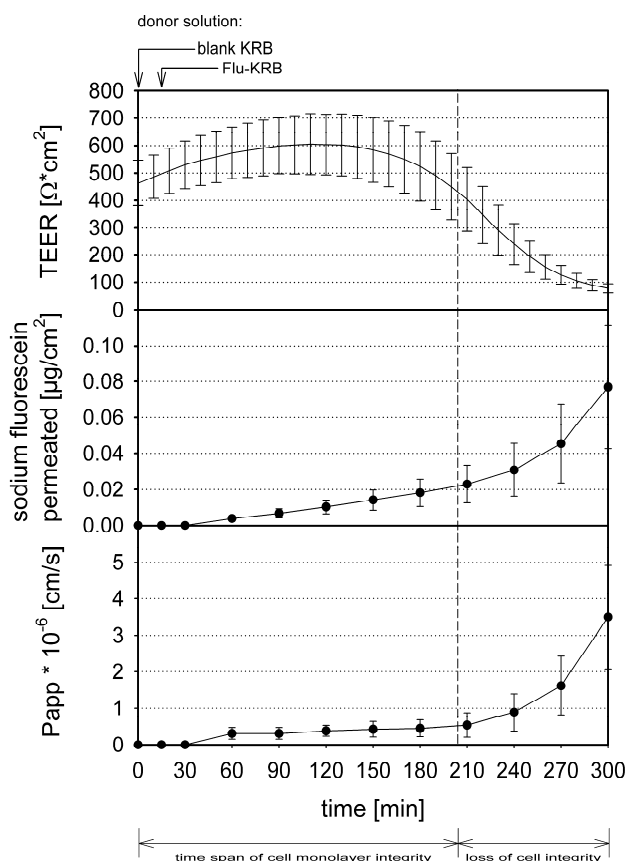


Figure 3-4 Time course of TEER, fluorescein transport and apparent permeability (P_{app}) as calculated from the latter. Shown are mean \pm SD of $n = 3$ experiments.

The finding of a value of $300 \Omega \times \text{cm}^2$ as the limit for paracellular tightness is in good agreement to the literature and seems to be valid also for other epithelial *in vitro* models [85]. A linear permeation pattern of sodium fluorescein was obtained although TEER did not remain on a constant level within the first three hours. The observation that certain differences in TEER are not reflected in the permeation profile is not an uncommon phenomenon for Caco-2 cells [86-88] and might partly be caused by an insufficient resolution of standard marker-flux measurement. Furthermore, it should be considered that mechanistically TEER measurement is a surrogate for ionic permeability and mainly based upon Na^+ permeability [80]. So, comparing the different methods to check paracellular

permeability it has to be considered that TEER may measure different properties of the tight junctions than flux studies do. In fact, the calculation of pore radii from permeability data by means of the Renkin function revealed a nonlinear correlation between pore size and TEER in rat alveolar cell monolayers [89]. Nevertheless, the concept of establishing a minimum TEER to be maintained throughout an experiment seems to be an adequate tool for in process control, provided that the interrelation between TEER and solute permeability has been elucidated before. So, according to instant results a time window of three hours is available for combined dissolution and permeation experiments with the revised basolateral setup. In comparison to that, for long-term Caco-2 experiments in culture plates, which are usually conducted using cell culture medium instead of buffer solutions, experimental times and monolayer integrity of up to six hours have been reported [33, 90]. The reason for this difference is attributed to the dynamic flow through character of the setup that implies stronger mechanical stress on the monolayer. On the other hand three hours are a sufficiently long period of time to study the performance of oral immediate release (IR) dosage forms of BCS class III and IV compounds which is the main focus of the apparatus. Next to that, this precondition fits well to the reported human small intestinal transit time of 3 ± 1 hour [91].

3.7 Microscopic inspection of Caco-2 cells in comparison to TEER measurement

In this study it was aimed to elucidate if the change in electrical properties also leads to changes of the cellular morphology during the course of time that the cells are mounted inside the FTPC. Therefore, online TEER was recorded and either after two hours (high TEER) or after five hours (low TEER) the respective Transwell[®] was removed. For a closer analysis the

cells were fixed with 4 % formalin in phosphate buffer. Afterwards the nuclei were stained with hematoxylin and 4 μm cross-sections of the polyester membranes with the Caco-2 cells on top were prepared. Microscopic analysis of the cross-sections was done with a Leica DMRB upright microscope (Leica Microsystems GmbH, Wetzlar, Germany). As expected, TEER was still on a high level after two hours whereas after five hours inside the FTPC TEER of the respective Caco-2 cell monolayer decreased to a low value beneath $100 \Omega \times \text{cm}^2$ (Figure 3-5).

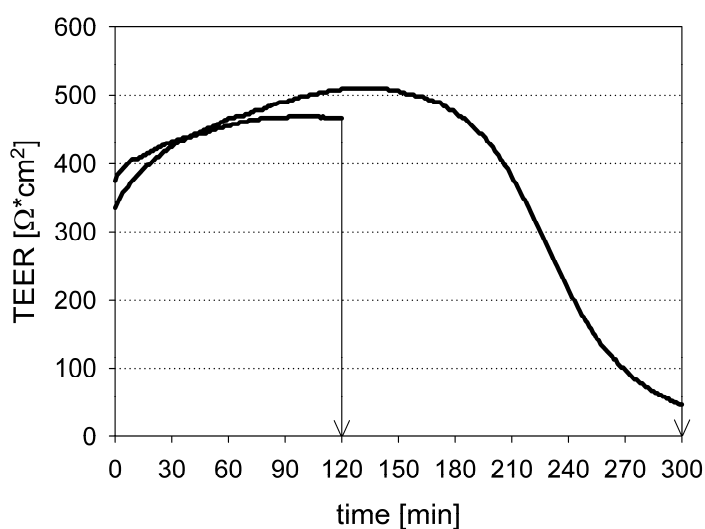


Figure 3-5 Course of TEER of two Caco-2 cell monolayers. Arrows indicate the times when the Transwell® supports were removed from the FTPC for microscopic analysis.

In agreement to the course of TEER there was no morphological difference between the cell monolayer after two hours inside the FTPC (Figure 3-6b) and a monolayer that has been fixed directly after cultivation (Figure 3-6a). In contrast to that the cells have shrunk and the interconnections between adjacent cells have loosened after a period of five hours inside the FTPC (Figure 3-6c). Furthermore, small cavities between the cells and the surface of the membrane could be detected at that stage.

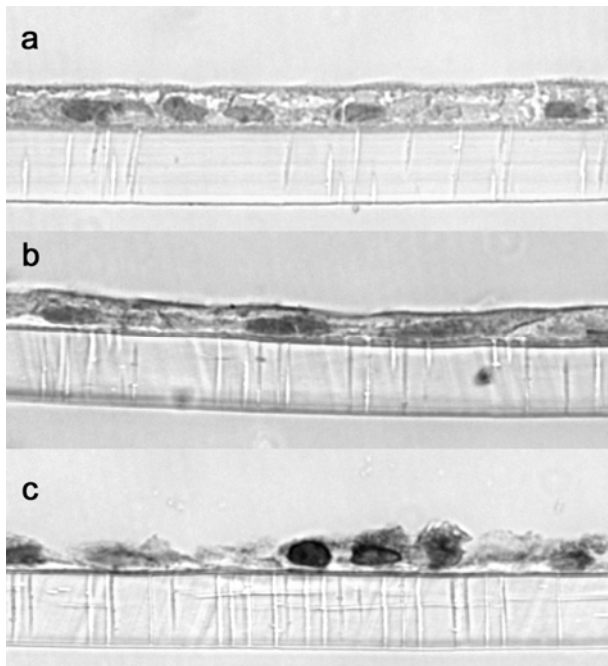


Figure 3-6 The figure shows cross-sections of three Caco-2 cell monolayers on top of polyester membranes (10 μm thickness, 0.4 μm pore size, Transwell[®] type 3460) at a 400 fold magnification, nuclei were stained with hematoxylin. **a:** A monolayer that has been fixed directly after cultivation serves as a control. **b:** This monolayer has been fixed after it was inside the FTPEC for two hours applying blank buffer with an apical flow rate of 1.0 ml/min. **c:** This picture shows the status of a third monolayer that was inside the FTPEC for five hours under the same conditions as described for figure 4b.

3.8 Online TEER measurement as a tool for the analysis of the influence of excipients on cell monolayer permeability

3.8.1 Introduction

In order to evaluate the performance of the new setup for continuous TEER measurement it was decided to make use of its known dependency on the extracellular concentration of Ca^{2+} . For tight monolayered epithelia it is known that a switch to Ca^{2+} free conditions causes a drop of TEER, resulting from an opening of the normally tight intercellular junctions. This

effect is even stronger if Ca^{2+} is actively depleted by means of a cation chelator, whereas after switching back to a Ca^{2+} containing medium TEER will recover again [92]. The velocity of resealing of the tight junctions was pointed out to be dependent on the time that the cells were kept in the status of Ca^{2+} depletion before [93]. In the vast majority of such studies the Ca^{2+} depletion was performed on both sides of the respective cell monolayer. Later on, a study by Noach et al. demonstrated that Caco-2 cells react much more sensitively to the application of EDTA from the basolateral side than from the apical side [94]. However, in our experiments Ca^{2+} depletion was performed only from the apical side as this is the scenario that is of *in vivo* relevance.

3.8.2 Buffer solutions

EDTA solutions contained 2, 3, 6 or 8 mM EDTA next to 5 $\mu\text{g/ml}$ sodium fluorescein and were prepared without addition of Ca^{2+} and Mg^{2+} (Flu-EDTA). The changes in osmolality, which were caused by the addition of EDTA and the omission of the divalent ions, were compensated to the calculative value of KRB using NaCl. Isoosmolality of all solutions of 308 ± 4 mosmol/kg was controlled via freezing point depression (Semi-micro Osmometer, Knauer GmbH, Berlin, Germany). All solutions were adjusted to pH 7.4 in order to exclude influences on solute transport or electric measurement caused by a pH gradient between the apical and the basolateral compartment.

3.8.3 Experimental procedure

In order to analyze the modulation of cell monolayer tightness, the donor medium was switched to a Flu-EDTA solution for a certain period of time to illustrate some permeation enhancing effect on the monolayer and back again to Flu-KRB. Switching between the different donor solutions was feasible without interruption of the apical flow and without aspiration of any air bubbles due to the discontinuous suction of the membrane pump. In preliminary tests a time frame of 45 minutes for application of Flu-EDTA solutions was found to be suitable for the experiments. Starting with the highest concentration of 8 mM a step by step reduction of the EDTA concentration was conducted in the experiments shown in Figure 3-7.

3.8.4 Results

The application of high EDTA concentrations of 8 and 6 mM led to a pronounced drop of TEER and after switching back to Ca²⁺-containing Flu-KRB solution no stabilisation was reached. In agreement with the course of TEER the permeability of sodium fluorescein increased after application of the Flu-EDTA solutions and no reduction or slowing down of this process after Ca²⁺ restoration was observed. In coincidence with the ongoing drop of TEER the cumulative amount of sodium fluorescein showed a parabolic profile, corroborating a continuously increasing permeability of the monolayer. Reduction of the EDTA concentration to 3 and 2 mM led to a different picture. After the EDTA induced drop, TEER recovered as soon as Ca²⁺ was available in the apical medium again. Within the period of TEER recovery the cumulative amount of permeated sodium fluorescein increased linearly and permeability persisted at an almost constant level. Only when the expected time span of cell monolayer

integrity ended after about 3.5 hours inside the FTPEC epithelial permeability increased again.

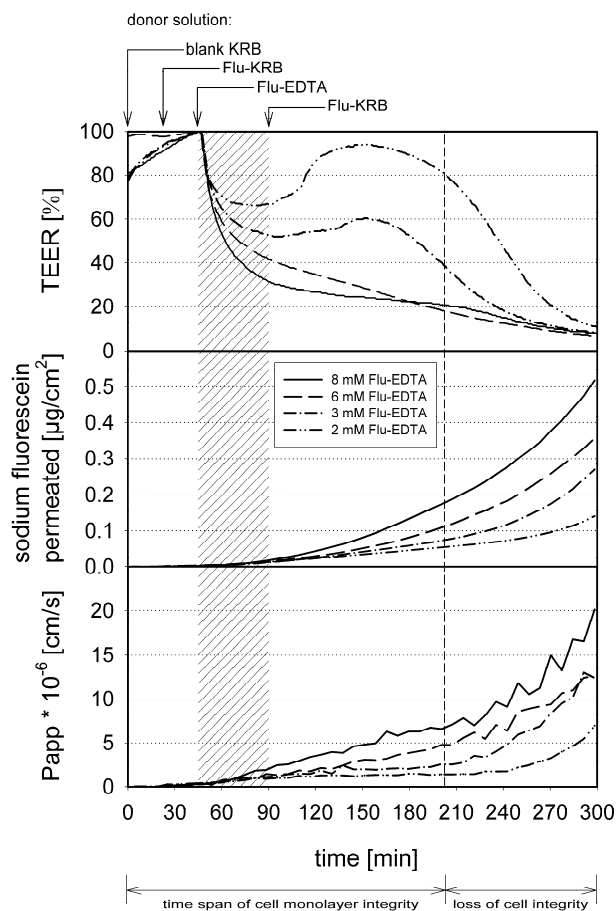


Figure 3-7 Application of 8, 6, 3 and 2 mM EDTA containing buffer for a time interval of 45 minutes and subsequent return to KRB. All solutions applied later than 15 minutes after the start of an experiment contained 5 µg/ml of sodium fluorescein (Flu-KRB; Flu-EDTA). TEER values were normalized to the maximum value of the respective experiment in order to allow for a better comparability of the EDTA effect. The figure shows single data for each EDTA concentration.

3.8.5 Recovery of TEER after repeated Ca^{2+} switching

Afterwards, a repeated switching between Flu-EDTA and Flu-KRB solution was evaluated. As can be seen in Figure 3-8, switching between 8 mM Flu-EDTA and Flu-KRB for four times with an exposure to the Ca^{2+} chelator for only ten minutes each time led to a stepwise decrease of TEER and was followed by a decreasing capability of the cells to recover again. Despite that, the cumulative amount of permeation showed a parabolic shape and the flux over the monolayer increased steadily with a tendency to increase above average after three hours, as already seen in the previous experiments.

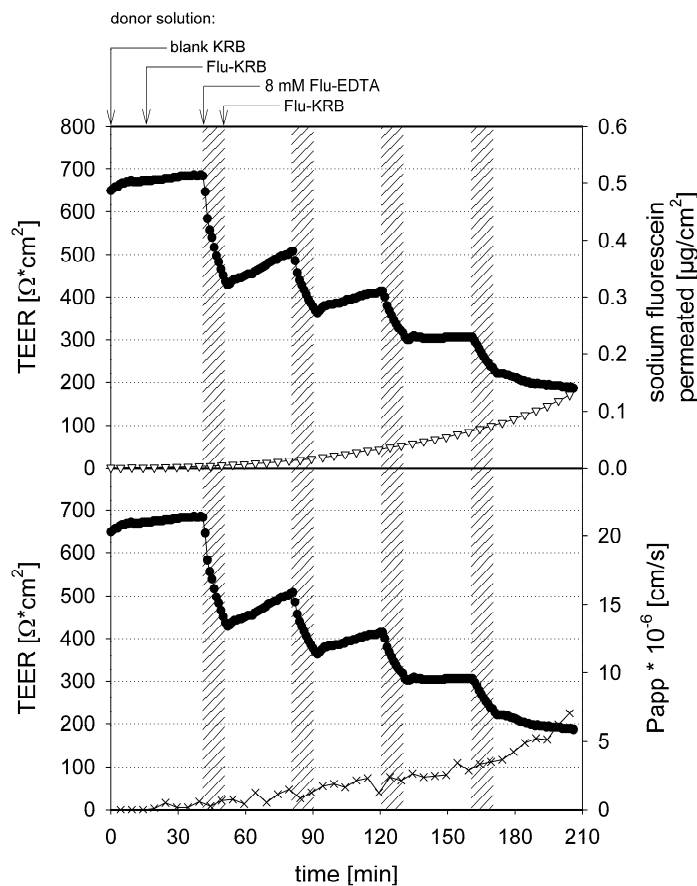


Figure 3-8 Change in cell monolayer leakiness following four 10 minutes applications (hatched areas) of 8 mM EDTA assessed during the course of the same experiment.

3.8.6 Discussion

EDTA induced Ca^{2+} depletion from the apical compartment led to a pronounced drop of TEER. Synopsis of the experiments with identical procedure and an application of 8 to 2 mM EDTA for 45 minutes revealed a concentration dependent decrease of TEER within the time of exposure to the chelating agent. Comparison of the respective permeability that was reached after 200 minutes, the time that the cell monolayer integrity was shown to be limited to, also reflected the rank order of EDTA concentrations (Figure 3-7). Next to that, a dose dependency was found for the recovery of TEER after switching back to Flu-KRB solution. Whereas after application of higher EDTA concentrations (8 and 6 mM) for 45 minutes, the decrease of TEER was irreversible, the exposure to lower EDTA concentrations (3 and 2 mM) was followed by a recovery of the TEER (Figure 3-7). A closer look upon sodium fluorescein permeation throughout the periods of TEER recovery revealed a linear increase of the permeated amount and a constant permeability on a higher level in comparison to an unaffected cell monolayer. It was concluded that recovery of TEER in this case did not lead to a complete resealing but to a conservation of the current permeability of the Caco-2 monolayer for sodium fluorescein. In this context a study by Watson et al. who have introduced a novel tool that allows detection of graded changes in paracellular permeability provided helpful mechanistic insight [95]. By means of simultaneous permeability screening of a series of polyethylene glycol oligomers (PEG-profiling) the authors pointed out that upon Ca^{2+} chelation the cell monolayer lost its ability for size discrimination. Functional modelling suggested an increase in pore size as the underlying mechanism. The evaluation of PEG-profiling with different EDTA concentrations conducted by the same authors did not result in a clear gradation for the effect of Ca^{2+} depletion. This might be caused by the fact that the Ca^{2+} chelator was also added to the highly sensitive basolateral

side of the cell monolayer. Higher EDTA concentrations (8 and 6 mM) did not lead to a recovery but showed a continuously decreasing TEER. In agreement to that finding, the permeated amount of sodium fluorescein showed a nonlinear growth and the permeability was increasing steadily. So it was concluded that the process of pore size increase initiated by EDTA in these cases could not be stopped by means of Ca^{2+} reconstitution anymore.

In comparison to flux studies TEER measurement is the more sensitive method with a high temporal resolution [96]. However, this advantage reveals its full value only in case of continuous recording which could be pointed out by repeated switches to 8 mM Flu-EDTA and back to Ca^{2+} containing buffer (Figure 3-8). In contrast to the instantaneous and sensitive response of TEER upon the repeated short term EDTA application the permeability of sodium fluorescein followed with a certain delay and did not show a gradation. It was concluded that the time periods of 30 minutes in between the single EDTA bolus applications were too short for detection of an equilibration of the flux.

In consequence the different methods to characterize paracellular permeability of an epithelial cell monolayer provide complementary information and have to be interpreted cautiously. In order to get a complete picture of the state of paracellular permeability, combinations of TEER and diffusion measurement would be required [75]. Furthermore, it has to be considered that membrane permeation even of hydrophilic drugs may not solely be based upon one single paracellular mechanism. Sodium fluorescein, which longtime has been regarded as the standard marker dye for paracellular transport, seems to be transported actively in case of application of a pH gradient between the apical and the basolateral compartment and was stated to be substrate of a proton coupled

monocarboxylic anion transporter [97, 98]. Therefore, in this study all experiments have been carried out under iso-pH conditions of pH 7.4 on both sides of the cell monolayer which is supposed to limit epithelial transport to the paracellular route. The TEER of a Caco-2 cell monolayer grown on a permeable support is highly sensitive to surrounding conditions like buffer changes and temperature drops. Thus, equilibration periods under controlled conditions for at least 15 minutes after each manipulation are required in order to obtain reliable TEER values [75]. Here our setup offers advantages by its design as a flow through system providing a seamless transition of the donor composition inside the apical compartment. Due to the relatively high heat capacity of polyetheretherketone (PEEK) used to manufacture the FTPC and submersion into a preheated water bath, an equilibration is only necessary at the start of an experiment. Finally, the availability of only two single TEER values, one measured before and one after an experiment in absence of constant external conditions, are to be regarded as insufficient. Continuous TEER measurement inside the FTPC is much more reliable and less error prone.

3.8.7 Conclusions

Cell monolayer integrity and, regarded with a closer focus, the actual status of the paracellular permeability are critical parameters that should be controlled during a transport experiment across Caco-2 cells. This applies especially in case of intentional manipulation of the cell monolayer permeability as purposed with the apparatus. By means of continuous TEER measurement a sensitive tool for online monitoring of the barrier status of Caco-2 cell monolayers has been implemented into the apparatus for combined measurement of dissolution and permeation. The

instantaneous availability of the respective TEER profile to each experiment provides an adequate in-line control and points out the validity of the experimental data. Next to that, the informative value of the online and on-site TEER measurement is much higher in comparison to the prior situation, when TEER could only be measured outside the FTPC, before and after an experiment. However, it has to be considered that TEER measurement cannot provide a complete picture of the paracellular permeability. Therefore, a careful interpretation of the data is essential to obtain a deeper insight into the changes at the cell monolayer. The novel feature will allow investigating advanced formulation approaches for oral drug delivery and it helps understanding the interplay of drugs and excipients with the intestinal barrier. Finally it aims for the establishment of rationales for the incorporation of permeation enhancers or combinations of excipients with additional physicochemical or biological targets such as efflux pumps and gut wall associated metabolic enzymes into solid oral drug formulations.

4 Proof of concept using the BCS class IV compound furosemide

4.1 Permeation of furosemide in the revised apparatus

After successful adaption of the apparatus for the analysis of low permeable compounds, installation of online TEER measurement and the analysis of excipient effects on cell monolayer integrity, it was decided to reassess the BCS class IV compound furosemide with the revised equipment under the same conditions as described in chapter 2.2.3. In this study it was of particular interest to clarify if the compound now featured a reasonable permeation. Therefore, Lasix[®] 40 mg IR tablets were analyzed in two sets of experiments applying either a single tablet (Figure 4-1) or two of the tablets at one time inside the flow through dissolution cell (Figure 4-2).

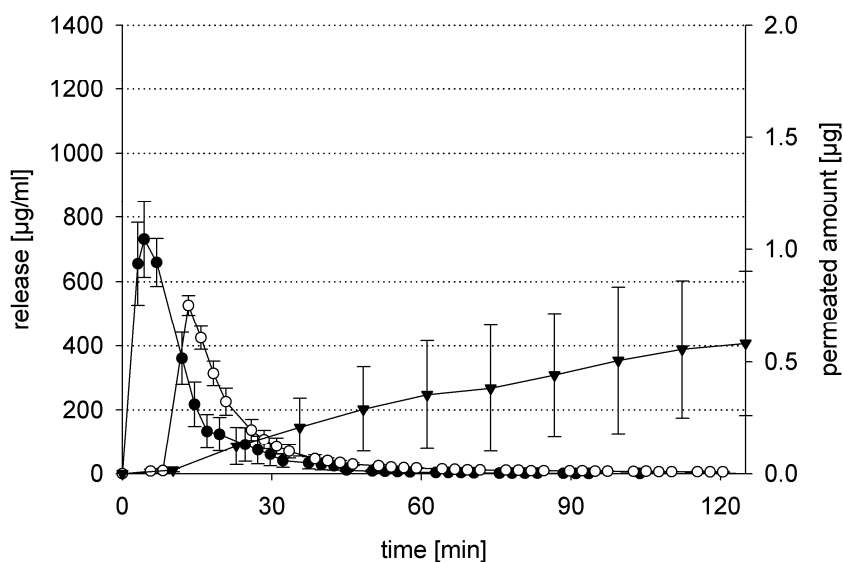


Figure 4-1 Analysis of single Lasix[®] 40 mg IR tablets. Closed circles (●) represent the furosemide concentration measured at sampling port D, open circles (○) the concentrations at port A and triangles down (▼) point out the amount of drug that permeated into the basolateral compartment (n = 3).

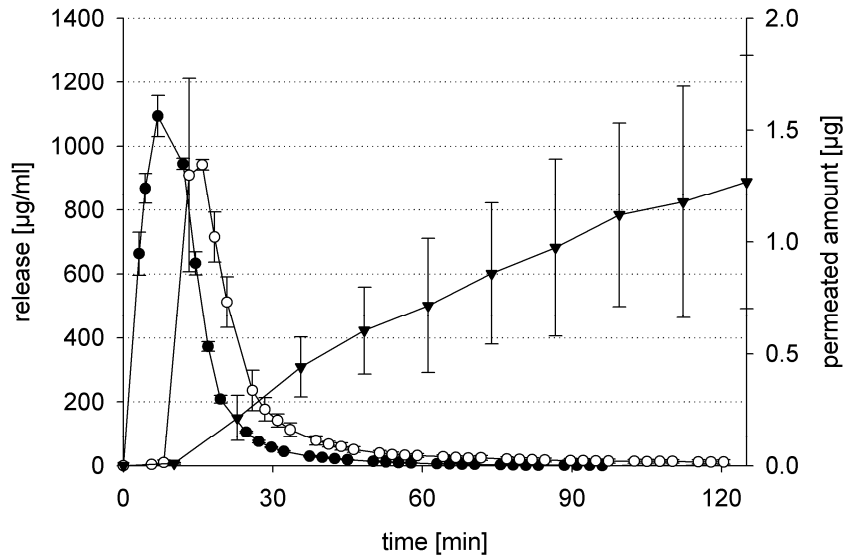


Figure 4-2 Analysis of 2 Lasix[®] 40 mg IR tablets inside the dissolution cell. Closed circles (●) represent the furosemide concentration measured at sampling port D, open circles (○) the concentrations at port A and triangles down (▼) point out the amount of drug that permeated into the basolateral compartment (n = 3).

Next to the drug concentrations the course of TEER was recorded pointing out that the barrier function of the cell monolayers was maintained throughout the experiments (Figure 4-3, Figure 4-4).

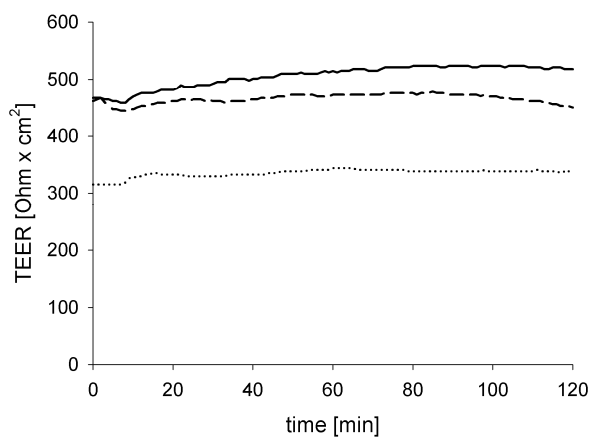


Figure 4-3: Course of TEER inside the FTPC during the experiments analyzing single Lasix[®] tablets.

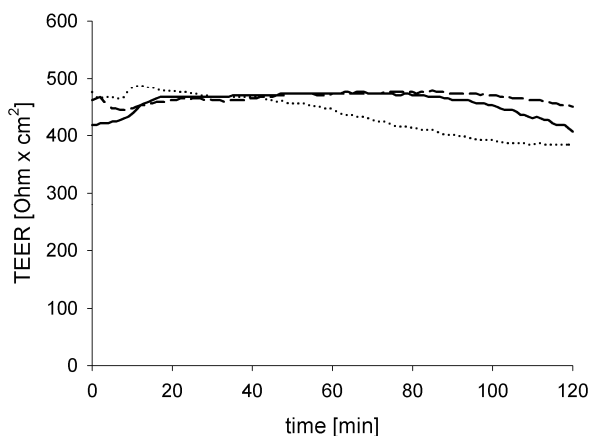


Figure 4-4: Course of TEER inside the FTPC during the experiments analyzing 2 Lasix[®] tablets in each experiment.

Comparing the AUCs of the curves for one and two tablets an approximately twofold increase was found at the apical and the basolateral port (Table 4-1).

	AUC 1 tablet	AUC 2 tablets	Ratio
D	9314	15549	1.67
A	7292	14089	1.93
B	40	86	2.15

Table 4-1 Comparison of the AUCs for the dissolution and permeation experiments using either a single or two Lasix[®] tablets at the same time.

The weaker dose linearity calculated for port D might be attributed to the rapid release of the compound from the Lasix[®] formulation leading to a pronounced peak in the dissolution profile which was difficult to describe with the available number of sampling points. With $0.58 \pm 0.32 \mu\text{g}$ for one tablet and $1.27 \pm 0.57 \mu\text{g}$ for two tablets, the absolute amounts of drug that permeated across the cell monolayer were very low. Relative to the amount of drug that cumulatively appeared at the apical port a percentage

of 0.0080 % for the single tablet and 0.0090 % for two tablets was calculated. In comparison to approximately 0.35% of drug permeation for propranolol IR tablets (chapter 1.4.1) this revealed a 44 to 39 times lower extent of permeation of furosemide. In conclusion this study demonstrated that next to the analysis of fluorescent dyes the revised apparatus allows the analysis of formulations containing low permeable compounds which is a prerequisite for the future evaluation of e.g. formulation factors, excipients and dissolution media on the performance of BCS class III and IV compounds.

5 Summary and outlook

In the present work several achievements have been made that advance the applicability of the apparatus for combined measurement of dissolution and permeation of solid oral dosage forms. In a first step, the challenge to allow the analysis of low permeable compounds has been addressed. In this process the basolateral compartment has been revised which provided for an abolishment of the multiple subdivisions, the minimization of the acceptor volume and a simplification of the handling. Next to that, an intrinsic carry-over effect at the valve of the automation module has been identified as a major cause for the unexpectedly high and inconsistent concentrations of furosemide measured at the basolateral sampling port. This issue could be circumvented by installation of a second valve for basolateral sampling separating the routes for high concentration assessment at port D and A from the much lower concentrations to be detected at port B. The proper function of the revised apparatus was pointed out using sodium fluorescein and rhodamine 123 as marker compounds for low permeability. Next to the adaptation of the apparatus for the analysis for low permeable compounds it was aimed to provide for the option to monitor cell monolayer integrity inside the FTPC. This was realized by implementation of online TEER measurement which was pointed out to be a valuable method supporting and completing the results from marker flux measurement. Applying both methods, the viability of the Caco-2 cell monolayers inside the revised apparatus was determined to roughly 3.5 hours. In the next step it was evaluated if the novel feature of online TEER measurement could also be used as a tool to analyze the influence of excipients on cell monolayers. In this context the known relationship between Ca^{2+} availability and functional tight junctions was utilized applying EDTA solution in the apical compartment for certain periods of time. Simultaneously the flux of the paracellular marker sodium

fluorescein was measured and online TEER was recorded revealing interesting relations and advantages of the complementary methods and encouraging testing online TEER measurement in an approach that uses excipients incorporated into complete solid oral dosage forms as a next step. In this context two approaches might be of interest. At first a compound that is substrate of epithelial efflux transport like furosemide or digoxin could be coadministered with an efflux inhibitor like TPGS at different doses. Digoxin might be of interest, as for this compound a marketed soft gelatin capsule is available in the US (Lanoxicaps™). Absorption of digoxin from this formulation is reported to be 90 - 100%, whereas standard digoxin tablets provide a bioavailability of 60 to 80% (<http://www.drugs.com/pro/lanoxicaps.html>). In a second step it could also be interesting to evaluate the most promising compounds proposed by Whitehead et al. [30, 31]. Although the mechanism of permeation enhancement for some of the compounds that have been elucidated in those studies is unknown, the enhancers and strategies to circumvent toxicity proposed by the authors might be interesting to be evaluated using the apparatus for combined measurement of dissolution and permeation.

A further point of interest is the implementation of cell culture compatible biorelevant dissolution media aiming for the estimation of a potential food effect. In contrast to the standard procedure that uses the dissolution profile in USP apparatus 2 as a criterion, the apparatus allows to also consider the successive and maybe even more significant criterion of permeation next to analysis of the dissolution profile.

So, the field of combined dissolution and permeation testing definitively offers further interesting opportunities for research. Practical relevance of such efforts will be provided by the opportunity to analyze complete oral dosage forms.

6 Annexes

6.1 List of abbreviations

ADME	absorption, distribution, metabolism and elimination
API	active pharmaceutical ingredient
AUC	area under the curve
BCS	biopharmaceutical classification system
BE	bioequivalence
BNC	bayonet Neill-Concelman
conc.	concentration
CYP	cytochrome P
EDTA	Ethylenediaminetetraacetic acid disodium salt
e.g.	exempli gratia
et al.	et alii
ER	extended release
EVOM	epithelial volt ohm meter
FDA	Food and Drug Administration
Flu-EDTA	Krebs Ringer buffer containing sodium fluorescein and EDTA
Flu-KRB	Krebs Ringer buffer containing sodium fluorescein
FTPC	flow through permeation cell
HPLC	high pressure liquid chromatography
IR	immediate release
IVIVC	in vitro-/ in vivo correlation
KRB	Krebs Ringer buffer
LOD	limit of detection
LOQ	limit of quantification
no.	number
PAMPA	parallel artificial membrane permeability assay
P_{app}	apparent permeability coefficient

PEEK	polyetheretherketone
PEG	polyethylene glycol
P-gp	P-glycoprotein
PMT-FL	photomultiplier tube for fluorescence detection
SIA	sequential injection analysis
SD	standard deviation
TEER	transepithelial electrical resistance
TPGS	tocopheryl polyethylene glycol succinat
USP	United States Pharmacopoeia
UV	ultra violet light
VIS	visible light
WHO	World Health Organization

6.2 Allocation of the ports at the SIA valves

6.2.1 8-port valve

Port number	Port appellation
1	WASTE
2	UV VIS
3	PMT-FL
4	DISSOLUTION
5	APICAL
6	BASOLATERAL
7	KRB SUPPLY
8	AUTOSAMPLER

6.2.2 6-port valve

Port number	Port appellation
1	Müll
2	Buffer
3	Akzeptorkompartiment
4	Probensammler
5	Abfall
6	6

6.3 Programming codes for SIA automation

6.3.1 SIA programs for furosemide

Main routine furosemide

Hardware Settings Wavelength 1 (nm) 275
Hardware Settings Wavelength 2 (nm) 274
Hardware Settings Wavelength 3 (nm) 344
Hardware Settings Wavelength 4 (nm) 360

autosampler Command: Set port 5
Spectrometer Reference Scan
Delay (sec) 145

Insert File C:\Programme\WINFIA 5.0\Marco\Furosemid\dissolution_flowrate 10.fia
Insert File C:\Programme\WINFIA 5.0\Marco\Furosemid\dissolution_flowrate 10.fia
Insert File C:\Programme\WINFIA 5.0\Marco\Furosemid\apical_flowrate 10.fia
Insert File C:\Programme\WINFIA 5.0\Marco\Furosemid\dissolution_flowrate 10.fia
Insert File C:\Programme\WINFIA 5.0\Marco\Furosemid\apical_flowrate 10.fia

Variable Define New sampos

sampos = 1

Insert File C:\Programme\WINFIA 5.0\Marco\Furosemid\basolateral_new_compartment
_new_valve.fia

sampos += 1

Loop Start (#) 40

Insert File C:\Programme\WINFIA 5.0\Marco\Furosemid\dissolution_flowrate 10.fia
Insert File C:\Programme\WINFIA 5.0\Marco\Furosemid\apical_flowrate 10.fia
Insert File C:\Programme\WINFIA 5.0\Marco\Furosemid\dissolution_flowrate 10.fia
Insert File C:\Programme\WINFIA 5.0\Marco\Furosemid\apical_flowrate 10.fia
Insert File C:\Programme\WINFIA 5.0\Marco\Furosemid\dissolution_flowrate 10.fia
Insert File C:\Programme\WINFIA 5.0\Marco\Furosemid\apical_flowrate 10.fia
Insert File C:\Programme\WINFIA 5.0\Marco\Furosemid\dissolution_flowrate 10.fia
Insert File C:\Programme\WINFIA 5.0\Marco\Furosemid\apical_flowrate 10.fia
Insert File C:\Programme\WINFIA 5.0\Marco\Furosemid\basolateral_new_compartment
_new_valve.fia

sampos += 1

Loop end

Subroutine: dissolution_flowrate 10.fia

Syringe Pump Valve In
 Syringe Pump Flowrate (microliter/sec) 500
 Syringe Pump Aspirate (microliter) 750
Multiposition Valve dissolution
 Syringe Pump Delay Until Done
 Syringe Pump Valve Out
 Syringe Pump Flowrate (microliter/sec) 50
 Syringe Pump Aspirate (microliter) 100
 Syringe Pump Delay Until Done
Multiposition Valve Waste
 Syringe Pump Flowrate (microliter/sec) 100
 Syringe Pump Dispense (microliter) 300
 Syringe Pump Delay Until Done
Multiposition Valve dissolution
 Syringe Pump Flowrate (microliter/sec) 10
 Syringe Pump Aspirate (microliter) 50
 Syringe Pump Delay Until Done
 Delay (sec) 1
Multiposition Valve UV- detector
 Syringe Pump Flowrate (microliter/sec) 1

Analyte New Sample
Analyte Name Dis
Spectrometer Absorbance Scanning
 Delay (sec) 1
 Syringe Pump Dispense (microliter) 300
 Syringe Pump Delay Until Done
 Spectrometer Stop Scanning

 Syringe Pump Flowrate (microliter/sec) 50
 Syringe Pump Empty
 Syringe Pump Delay Until Done

Subroutine apical_flowrate 10.fia

Syringe Pump Valve In
 Syringe Pump Flowrate (microliter/sec) 500
 Syringe Pump Aspirate (microliter) 800
Multiposition Valve apical
 Syringe Pump Delay Until Done
 Syringe Pump Valve Out
 Syringe Pump Flowrate (microliter/sec) 50
 Syringe Pump Aspirate (microliter) 150
 Syringe Pump Delay Until Done
Multiposition Valve Waste
 Syringe Pump Flowrate (microliter/sec) 100
 Syringe Pump Dispense (microliter) 400
 Syringe Pump Delay Until Done
Multiposition Valve apical
 Syringe Pump Flowrate (microliter/sec) 10
 Syringe Pump Aspirate (microliter) 50

Syringe Pump Delay Until Done
Delay (sec) 1
Multiposition Valve UV- detector
Syringe Pump Flowrate (microliter/sec) 10

Analyte New Sample
Analyte Name Api
Spectrometer Absorbance Scanning

Delay (sec) 1
Syringe Pump Dispense (microliter) 300
Syringe Pump Delay Until Done
Spectrometer Stop Scanning
Syringe Pump Flowrate (microliter/sec) 50
Syringe Pump Empty
Syringe Pump Delay Until Done

Subroutine: basolateral_new_compartment_new_valve.fia

Basolateral Pump Valve In
Basolateral Pump Flowrate (microliter/sec) 50
Basolateral Pump Aspirate (microliter) 325
Basolateral Pump Delay Until Done
Basolateral Pump Valve Out
Basolateral Valve Akzeptorkompartiment
Basolateral Pump Flowrate (microliter/sec) 10
Basolateral Pump Aspirate (microliter) 100
Basolateral Pump Delay Until Done
Basolateral Valve Abfall
Basolateral Pump Dispense (microliter) 125
Basolateral Pump Delay Until Done
Basolateral Valve 6
autosampler Wash
Basolateral Pump Flowrate (microliter/sec) 10
Basolateral Pump Aspirate (microliter) 25
Basolateral Pump Delay Until Done
Basolateral Valve Akzeptorkompartiment
Basolateral Pump Aspirate (microliter) 100
Basolateral Pump Delay Until Done
Basolateral Valve 6
Basolateral Pump Aspirate (microliter) 25
Basolateral Pump Delay Until Done
autosampler standard rack (sample #) 10
Delay (sec) 3
Basolateral Valve Probensammler
Basolateral Pump Flowrate (microliter/sec) 20
Basolateral Pump Dispense (microliter) 220
Basolateral Pump Delay Until Done
autosampler RACK 2 (sample #) = sampos
Delay (sec) 3
Basolateral Pump Dispense (microliter) 110
Basolateral Pump Delay Until Done
autosampler standard rack (sample #) 10

Delay (sec) 3
Basolateral Pump Valve In
Basolateral Pump Flowrate (microliter/sec) 50
Basolateral Pump Fill
Basolateral Pump Delay Until Done
Basolateral Pump Valve Out
Basolateral Pump Empty
Basolateral Pump Delay Until Done
Basolateral Pump Valve In
Basolateral Pump Fill
Basolateral Pump Delay Until Done
Basolateral Pump Valve Out
Basolateral Pump Empty
Basolateral Pump Delay Until Done
autosampler Wash

6.3.2 SIA programs for fluorescein and rhodamine

Spectrometer (PMT-FL) settings:

Integration time [ms]: 50

Sampling rate [Hz]: 4

Main routine fluorescein/ rhodamine

Variable Define New sampos
sampos = 1

Insert File C:\Programme\WINFIA 5.0\Marco\basolaterale Pumpe&Ventil\subroutinen\
Abfüllung basolateral in 96 well plate.fia

sampos += 1

Insert File C:\Programme\WINFIA 5.0\Marco\basolaterale Pumpe&Ventil\subroutinen\
Probenzug apical V50_Flow25_50ms_4Hz- neuer Probenzug_1500.fia
Delay (sec) 640

Insert File C:\Programme\WINFIA 5.0\Marco\basolaterale Pumpe&Ventil\subroutinen\
Abfüllung basolateral in 96 well plate.fia

sampos += 1

Insert File C:\Programme\WINFIA 5.0\Marco\basolaterale Pumpe&Ventil\subroutinen\
Probenzug apical V50_Flow25_50ms_4Hz- neuer Probenzug_1500.fia
Delay (sec) 340

Insert File C:\Programme\WINFIA 5.0\Marco\basolaterale Pumpe&Ventil\subroutinen\
Probenzug apical V50_Flow25_50ms_4Hz- neuer Probenzug_1500.fia
Delay (sec) 200

Loop Start (#) 60

Insert File C:\Programme\WINFIA 5.0\Marco\basolaterale Pumpe&Ventil\subroutinen\
Abfüllung basolateral in 96 well plate.fia

Insert File C:\Programme\WINFIA 5.0\Marco\basolaterale Pumpe&Ventil\subroutinen\
Probenzug apical V50_Flow25_50ms_4Hz- neuer Probenzug_1500.fia

sampos += 1

Delay (sec) 1540

Loop End

Subroutine: Probenzug apical V50_Flow25_50ms_4Hz- neuer Probenzug_1500.fia

Syringe Pump Valve In

Syringe Pump Flowrate (microliter/sec) 500

Syringe Pump Aspirate (microliter) 1500

Syringe Pump Delay Until Done

Syringe Pump Valve Out

Multiposition Valve apical

Syringe Pump Flowrate (microliter/sec) 15

Syringe Pump Aspirate (microliter) 100

Syringe Pump Delay Until Done

Multiposition Valve waste

Syringe Pump Flowrate (microliter/sec) 100

Syringe Pump Dispense (microliter) 200

Syringe Pump Delay Until Done

Multiposition Valve apical

Syringe Pump Flowrate (microliter/sec) 15

Syringe Pump Aspirate (microliter) 50

Syringe Pump Delay Until Done

Multiposition Valve PMT-FL

Syringe Pump Flowrate (microliter/sec) 25

Syringe Pump Empty

Analyte New Sample

Analyte Name apical

PMT Start Scans

Syringe Pump Delay Until Done

PMT Stop Scans

Subroutine: Abfüllung basolateral in 96 well plate

Basolateral Pump Valve In
 Basolateral Pump Flowrate (microliter/sec) 50
 Basolateral Pump Aspirate (microliter) 325
 Basolateral Pump Delay Until Done

Basolateral Pump Valve Out
 Basolateral Valve Akzeptorkompartiment
 Basolateral Pump Flowrate (microliter/sec) 10
 Basolateral Pump Aspirate (microliter) 100
 Basolateral Pump Delay Until Done
 Basolateral Valve Abfall
 Basolateral Pump Dispense (microliter) 125
 Basolateral Pump Delay Until Done

Basolateral Valve 6
 autosampler Wash
 Basolateral Pump Flowrate (microliter/sec) 10
 Basolateral Pump Aspirate (microliter) 25
 Basolateral Pump Delay Until Done

Basolateral Valve Akzeptorkompartiment
 Basolateral Pump Aspirate (microliter) 100
 Basolateral Pump Delay Until Done

Basolateral Valve 6
 Basolateral Pump Aspirate (microliter) 25
 Basolateral Pump Delay Until Done
 autosampler standard rack (sample #) 10
 Delay (sec) 3

Basolateral Valve Probensammler
 Basolateral Pump Flowrate (microliter/sec) 20
 Basolateral Pump Dispense (microliter) 220
 Basolateral Pump Delay Until Done
 autosampler RACK 4 (sample #) = sampos
 Delay (sec) 3
 Basolateral Pump Dispense (microliter) 110
 Basolateral Pump Delay Until Done
 autosampler standard rack (sample #) 10
 Delay (sec) 3

Basolateral Pump Valve In
 Basolateral Pump Flowrate (microliter/sec) 50
 Basolateral Pump Fill
 Basolateral Pump Delay Until Done

Basolateral Pump Valve Out
 Basolateral Pump Empty
 Basolateral Pump Delay Until Done

Basolateral Pump Valve In
 Basolateral Pump Fill
 Basolateral Pump Delay Until Done

Basolateral Pump Valve Out
 Basolateral Pump Empty
 Basolateral Pump Delay Until Done
 autosampler Wash

6.3.3 Test routine for the multiposition-valve

Spectrometer (PMT-FL) settings:
Integration time [ms]: 80
Sampling rate [Hz]: 4

Main routine

Loop Start (#) 60

Insert File C:\Programme\WINFIA 5.0\Marco\Propranolol\probenzug 25\Probenzug
dissolution 25- neuer Propenzug.fia
Insert File C:\Programme\WINFIA 5.0\ Marco\Propranolol\probenzug 25\Probenzug
apical 25- neuer Probenzug.fia

Loop End

Subroutine: Probenzug dissolution 25- neuer Propenzug.fia

Syringe Pump Valve In
Syringe Pump Flowrate (microliter/sec) 250
Syringe Pump Aspirate (microliter) 1000
Syringe Pump Delay Until Done

Syringe Pump Valve Out
Multiposition Valve dissolution
Syringe Pump Flowrate (microliter/sec) 100
Syringe Pump Aspirate (microliter) 50
Syringe Pump Delay Until Done

Multiposition Valve waste
Syringe Pump Flowrate (microliter/sec) 200
Syringe Pump Dispense (microliter) 100
Syringe Pump Delay Until Done

Multiposition Valve dissolution
Syringe Pump Flowrate (microliter/sec) 25
Syringe Pump Aspirate (microliter) 25
Syringe Pump Delay Until Done

Multiposition Valve PMT-FL
Syringe Pump Flowrate (microliter/sec) 50
Syringe Pump Empty

Analyte New Sample
Analyte Name dissolution
PMT Start Scans
Syringe Pump Delay Until Done
PMT Stop Scans

Subroutine: Probenzug apical 25- neuer Probenzug.fia

Syringe Pump Valve In
 Syringe Pump Flowrate (microliter/sec) 500
 Syringe Pump Aspirate (microliter) 1000
 Syringe Pump Delay Until Done

Syringe Pump Valve Out
 Multiposition Valve apical
 Syringe Pump Flowrate (microliter/sec) 15
 Syringe Pump Aspirate (microliter) 100
 Syringe Pump Delay Until Done

 Multiposition Valve waste
 Syringe Pump Flowrate (microliter/sec) 200
 Syringe Pump Dispense (microliter) 200
 Syringe Pump Delay Until Done

 Multiposition Valve apical
 Syringe Pump Flowrate (microliter/sec) 15
 Syringe Pump Aspirate (microliter) 25
 Syringe Pump Delay Until Done

 Multiposition Valve PMT-FL
 Syringe Pump Flowrate (microliter/sec) 50
 Syringe Pump Empty

Analyte New Sample
Analyte Name apical
PMT Start Scans
Syringe Pump Delay Until Done
PMT Stop Scans

6.4 Autosampler configuration

Configuration of the autosampler rack for sampling into HPLC vials:

Name of rack:	RACK 2
Number of rows:	3
Number of columns:	13
X Position of Sample #1 (mm):	75
Y Position of Sample #1 (mm):	19
Delta X Position of Samples in rack (mm):	15
Delta Y Position of Samples in rack (mm):	18
Up Position (mm):	50
Down Position (mm):	117

Configuration of the autosampler rack for sampling into 96 well plates:

Name of rack:	RACK 4
Number of rows:	12
Number of columns:	8
X Position of Sample #1 (mm):	76
Y Position of Sample #1 (mm):	23
Delta X Position of Samples in rack (mm):	9
Delta Y Position of Samples in rack (mm):	9
Up Position (mm):	50
Down Position (mm):	142

6.5 PEEK adapter for electrode plugs

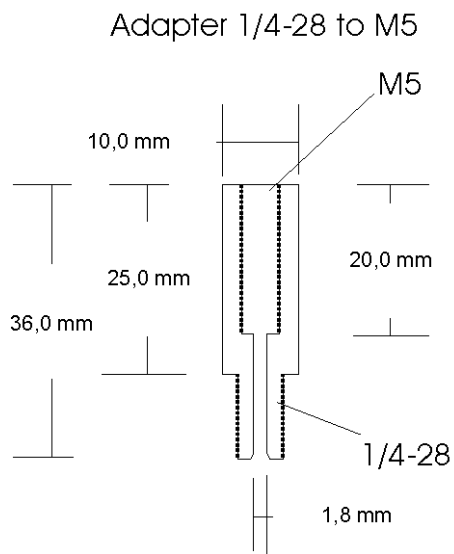


Figure 6-1 Detail drawing of the PEEK adapter for installation of wiring and plugs of electrodes for online TEER measurement inside the FTPC.

7 Curriculum vitae

personal details

name	Marco Mündörfer
date of birth	15.09.1979
place of birth	Karlsruhe, Germany

education

1986 – 1990	Grundschule Aue
1990 – 1999	Markgrafen-Gymnasium Durlach

public service

1999 – 2000	Arbeiterwohlfahrt Karlsruhe
-------------	-----------------------------

university studies

October 2000 – March 2005	Albert-Ludwigs-Universität, Freiburg, study of Pharmacy
------------------------------	--

internships

May 2005 – October 2005	Department of Biopharma-Operations, Manufacturing Science, Boehringer-Ingelheim Pharma GmbH, Biberach / Riss
----------------------------	--

November 2005 – April 2006	Elisabeth-Apotheke, Dresden
-------------------------------	-----------------------------

professional qualification

June 2006	Registration as a pharmacist
-----------	------------------------------

work experience

July 2006 – October 2006	Ludwig-Maximilians-Universität, Munich, scientific employee
-----------------------------	--

PhD thesis

January 2007 – April 2010	Saarland University, Saarbrücken, Department of Biopharmaceutics and Pharmaceutical Tech- nology
------------------------------	--

8 List of publications

Research paper:

Muendoerfer, M., U.F. Schaefer, P. Koenig, J.S. Walk, P. Loos, S. Balbach, T. Eichinger, and C.M. Lehr, Online monitoring of transepithelial electrical resistance (TEER) in an apparatus for combined dissolution and permeation testing. *Int J Pharm*, 2010. 392(1-2): p. 134-40.

Posters:

Motz, S.A., M. Muendoerfer, U.F. Schaefer, and C.-M. Lehr, Automated permeability assessment of furosemide tablets combining a flow through dissolution cell and Caco-2 monolayers. 3rd Pharmaceutical Sciences World Congress, April 20 – 25, 2007, Amsterdam, The Netherlands

Muendoerfer, M., J. S. Walk, S. Balbach, T. Eichinger, C. Korn, P. Loos, U. F. Schaefer, C.-M. Lehr, Monitoring the integrity of Caco-2 cell monolayers by continuous TEER measurement in the flow through permeation cell (FTPC), Berlin III – Sanofi-Aventis Global CMC Conference 2009, January 2009, Budapest, Hungary

Muendoerfer, M., J. S. Walk, S. Balbach, T. Eichinger, C. Korn, P. Loos, U. F. Schaefer, C.-M. Lehr, Continuous survey of Caco-2 cell monolayer integrity inside the Flow Through Permeation Cell using online TEER measurement, 8th International Conference and Workshop on Biological Barriers – in vitro Tools, Nanotoxicology, and Nanomedicine, March 21 – April 01, 2010, Saarbrücken, Germany

9 References

- [1] Food and Drug Administration, G.f.I., Dissolution Testing of Immediate Release Solid Oral Dosage Forms. 1997, Food and Drug Administration: Rockville, MD. p. 17.
- [2] Amidon, G.L., H. Lennernas, V.P. Shah, and J.R. Crison, A theoretical basis for a biopharmaceutic drug classification: the correlation of in vitro drug product dissolution and in vivo bioavailability. *Pharmaceutical Research*, 1995. 12(3): p. 413-20.
- [3] Food and Drug Administration, G.f.I., Waiver of in vivo Bioavailability and Bioequivalence Studies for Immediate-Release Solid Oral Dosage Forms Based on a Biopharmaceutics Classification System. 2000, Food and Drug Administration: Rockville, MD.
- [4] Dickinson, P.A., W.W. Lee, P.W. Stott, A.I. Townsend, J.P. Smart, P. Ghahramani, T. Hammett, L. Billett, S. Behn, R.C. Gibb, and B. Abrahamsson, Clinical relevance of dissolution testing in quality by design. *The AAPS Journal*, 2008. 10(2): p. 380-90.
- [5] Food and Drug Administration, G.f.I., Extended Release Oral Dosage Forms: Development, Evaluation, and Application of In Vitro/In Vivo Correlations. 1997, Food and Drug Administration: Rockville, MD.
- [6] Buch, P., P. Langguth, M. Kataoka, and S. Yamashita, IVIVC in oral absorption for fenofibrate immediate release tablets using a dissolution/permeation system. *Journal of Pharmaceutical Sciences*, 2009. 98(6): p. 2001-9.
- [7] Blume, H.H. and B.S. Schug, The biopharmaceutics classification system (BCS): class III drugs - better candidates for BA/BE waiver? *European Journal of Pharmaceutical Sciences*, 1999. 9(2): p. 117-21.
- [8] Yu, L.X., G.L. Amidon, J.E. Polli, H. Zhao, M.U. Mehta, D.P. Conner, V.P. Shah, L.J. Lesko, M.L. Chen, V.H. Lee, and A.S. Hussain, Biopharmaceutics classification system: the scientific basis for biowaiver extensions. *Pharmaceutical Research*, 2002. 19(7): p. 921-5.
- [9] Jantratid, E., S. Prakongpan, G.L. Amidon, and J.B. Dressman, Feasibility of biowaiver extension to biopharmaceutics classification system class III drug products: cimetidine. *Clinical Pharmacokinetics*, 2006. 45(4): p. 385-99.
- [10] Polli, J.E., L.X. Yu, J.A. Cook, G.L. Amidon, R.T. Borchardt, B.A. Burnside, P.S. Burton, M.L. Chen, D.P. Conner, P.J. Faustino, A.A. Hawi, A.S. Hussain, H.N. Joshi, G. Kwei, V.H. Lee, L.J. Lesko, R.A. Lipper, A.E. Loper, S.G. Nerurkar, J.W. Polli, D.R. Sanvordeker, R. Taneja, R.S. Uppoor, C.S. Vattikonda, I. Wilding, and G. Zhang, Summary workshop report: biopharmaceutics classification system--implementation challenges and extension opportunities. *Journal of Pharmaceutical Sciences*, 2004. 93(6): p. 1375-81.
- [11] Polli, J.E., B.S. Abrahamsson, L.X. Yu, G.L. Amidon, J.M. Baldoni, J.A. Cook, P. Fackler, K. Hartauer, G. Johnston, S.L. Krill, R.A. Lipper, W.A. Malick, V.P. Shah, D. Sun, H.N. Winkle, Y. Wu, and H. Zhang, Summary workshop report: bioequivalence, biopharmaceutics classification system, and beyond. *The AAPS Journal*, 2008. 10(2): p. 373-9.
- [12] Gupta, E., D.M. Barends, E. Yamashita, K.A. Lentz, A.M. Harmsze, V.P. Shah, J.B. Dressman, and R.A. Lipper, Review of global regulations concerning

References

- biowaivers for immediate release solid oral dosage forms. *European Journal of Pharmaceutical Sciences*, 2006. 29(3-4): p. 315-24.
- [13] WHO expert committee on specifications for pharmaceutical preparations. Fortieth report Annex 8 Proposal to waive in vivo bioequivalence requirements for WHO Model List of Essential Medicines immediate-release, solid oral dosage forms. World Health Organization technical report series, 2006. 937: p. 391- 437.
- [14] WHO expert committee on specifications for pharmaceutical preparations. Fortieth report Annex 7 Multisource (generic) pharmaceutical products: guidelines on registration requirements to establish interchangeability. World Health Organization technical report series, 2006. 937: p. 1-461, back cover.
- [15] Wu, C.Y. and L.Z. Benet, Predicting drug disposition via application of BCS: transport/absorption/ elimination interplay and development of a biopharmaceutics drug disposition classification system. *Pharmaceutical Research*, 2005. 22(1): p. 11-23.
- [16] Benet, L.Z., G.L. Amidon, D.M. Barends, H. Lennernas, J.E. Polli, V.P. Shah, S.A. Stavchansky, and L.X. Yu, The use of BDDCS in classifying the permeability of marketed drugs. *Pharmaceutical Research*, 2008. 25(3): p. 483-8.
- [17] Artursson, P. and J. Karlsson, Correlation between oral drug absorption in humans and apparent drug permeability coefficients in human intestinal epithelial (Caco-2) cells. *Biochemical Biophysical Research Communications*, 1991. 175(3): p. 880-5.
- [18] Lennernäs, H., Animal data: The contributions of the Ussing Chamber and perfusion systems to predicting human oral drug delivery in vivo. *Advanced Drug Delivery Reviews*, 2007. 59(11): p. 1103-1120.
- [19] Artursson, P., Cell cultures as models for drug absorption across the intestinal mucosa. *Critical Reviews in Therapeutic Drug Carrier Systems*, 1991. 8(4): p. 305-30.
- [20] Hillgren, K.M., A. Kato, and R.T. Borchardt, In vitro systems for studying intestinal drug absorption. *Medicinal Research Reviews*, 1995. 15(2): p. 83-109.
- [21] Avdeef, A., *Absorption and Drug Development Solubility, Permeability, and Charge State*. 2003, New York: Wiley, J. 312.
- [22] Russell, W.M.S. and R.L. Burch, *The Principles of Humane Experimental Technique*. 1959.
- [23] Lennernas, H., S. Nylander, and A.L. Ungell, Jejunal permeability: a comparison between the ussing chamber technique and the single-pass perfusion in humans. *Pharmaceutical Research*, 1997. 14(5): p. 667-71.
- [24] Ungell, A.L., S. Nylander, S. Bergstrand, A. Sjoberg, and H. Lennernas, Membrane transport of drugs in different regions of the intestinal tract of the rat. *Journal of Pharmaceutical Sciences*, 1998. 87(3): p. 360-6.
- [25] Kansy, M., F. Senner, and K. Gubernator, Physicochemical high throughput screening: parallel artificial membrane permeation assay in the description of passive absorption processes. *Journal of Medicinal Chemistry*, 1998. 41(7): p. 1007-10.
- [26] Balimane, P.V. and S. Chong, Cell culture-based models for intestinal permeability: a critique. *Drug Discovery Today*, 2005. 10(5): p. 335-43.
- [27] Lipinski, C.A., Drug-like properties and the causes of poor solubility and poor permeability. *Journal of Pharmacological and Toxicological Methods*, 2000. 44(1): p. 235-49.

-
- [28] Mayersohn, M. and M. Gibaldi, New method of solid-state dispersion for increasing dissolution rates. *Journal of Pharmaceutical Sciences*, 1966. 55(11): p. 1323-4.
- [29] Flexner, C., Dual protease inhibitor therapy in HIV-infected patients: pharmacologic rationale and clinical benefits. *Annual Review of Pharmacology and Toxicology*, 2000. 40: p. 649-74.
- [30] Whitehead, K., N. Karr, and S. Mitragotri, Safe and Effective Permeation Enhancers for Oral Drug Delivery. *Pharmaceutical Research*, 2007: p. 1-7.
- [31] Whitehead, K., N. Karr, and S. Mitragotri, Discovery of synergistic permeation enhancers for oral drug delivery. *Journal of Controlled Release*, 2008. 128(2): p. 128-33.
- [32] Hidalgo, I.J., T.J. Raub, and R.T. Borchardt, Characterization of the human colon carcinoma cell line (Caco-2) as a model system for intestinal epithelial permeability. *Gastroenterology*, 1989. 96(3): p. 736-749.
- [33] Artursson, P., Epithelial transport of drugs in cell culture. I: A model for studying the passive diffusion of drugs over intestinal absorptive (Caco-2) cells. *Journal of Pharmaceutical Sciences*, 1990. 79(6): p. 476-82.
- [34] Bailey, C.A., P. Bryla, and A.W. Mallick, The use of the intestinal epithelial cell culture model, Caco-2, in pharmaceutical development. *Advanced Drug Delivery Reviews*, 1996. 22(1-2): p. 85-103.
- [35] Yee, S., In vitro permeability across Caco-2 cells (colonic) can predict in vivo (small intestinal) absorption in man--fact or myth. *Pharmaceutical Research*, 1997. 14(6): p. 763-6.
- [36] Dantzig, A.H. and L. Bergin, Uptake of the cephalosporin, cephalexin, by a dipeptide transport carrier in the human intestinal cell line, Caco-2. *Biochimica et Biophysica Acta (BBA) - Biomembranes*, 1990. 1027(3): p. 211-217.
- [37] Sambruy, Y., S. Ferruzza, G. Ranaldi, and I. De Angelis, Intestinal cell culture models: Applications in toxicology and pharmacology. *Cell Biology and Toxicology*, 2001. 17(4-5): p. 301-317.
- [38] Custodio, J.M., C.Y. Wu, and L.Z. Benet, Predicting drug disposition, absorption/elimination/transporter interplay and the role of food on drug absorption. *Advanced Drug Delivery Reviews*, 2008. 60(6): p. 717-33.
- [39] Pinto, M., S. Robine Leon, and M.D. Appay, Enterocyte-like differentiation and polarization of the human colon carcinoma cell line Caco-2 in culture. *Biology of the Cell*, 1983. 47(3): p. 323-330.
- [40] Lennernäs, H., K. Palm, U. Fagerholm, and P. Artursson, Comparison between active and passive drug transport in human intestinal epithelial (caco-2) cells in vitro and human jejunum in vivo. *International Journal of Pharmaceutics*, 1996. 127(1): p. 103-107.
- [41] Rubas, W., N. Jezyk, and G.M. Grass, Comparison of the permeability characteristics of a human colonic epithelial (Caco-2) cell line to colon of rabbit, monkey, and dog intestine and human drug absorption. *Pharmaceutical Research*, 1993. 10(1): p. 113-118.
- [42] Stewart, B.H., O.H. Chan, R.H. Lu, E.L. Reyner, H.L. Schmid, H.W. Hamilton, B.A. Steinbaugh, and M.D. Taylor, Comparison of intestinal permeabilities determined in multiple in vitro and in situ models: Relationship to absorption in humans. *Pharmaceutical Research*, 1995. 12(5): p. 693-699.

References

- [43] Yamashita, S., Y. Tanaka, Y. Endoh, Y. Taki, T. Sakane, T. Nadai, and H. Sezaki, Analysis of drug permeation across Caco-2 monolayer: Implication for predicting in vivo drug absorption. *Pharmaceutical Research*, 1997. 14(4): p. 486-491.
- [44] Taipalensuu, J., H. Tornblom, G. Lindberg, C. Einarsson, F. Sjoqvist, H. Melhus, P. Garberg, B. Sjostrom, B. Lundgren, and P. Artursson, Correlation of gene expression of ten drug efflux proteins of the ATP-binding cassette transporter family in normal human jejunum and in human intestinal epithelial Caco-2 cell monolayers. *Journal of Pharmacology and Experimental Therapeutics*, 2001. 299(1): p. 164-70.
- [45] Hilgendorf, C., G. Ahlin, A. Seithel, P. Artursson, A.L. Ungell, and J. Karlsson, Expression of thirty-six drug transporter genes in human intestine, liver, kidney, and organotypic cell lines. *Drug metabolism and disposition: the biological fate of chemicals*, 2007. 35(8): p. 1333-40.
- [46] Sun, H., E.C. Chow, S. Liu, Y. Du, and K.S. Pang, The Caco-2 cell monolayer: usefulness and limitations. *Expert Opinion on Drug Metabolism & Toxicology*, 2008. 4(4): p. 395-411.
- [47] Brimer, C., J.T. Dalton, Z. Zhu, J. Schuetz, K. Yasuda, E. Vanin, M.V. Relling, Y. Lu, and E.G. Schuetz, Creation of polarized cells coexpressing CYP3A4, NADPH cytochrome P450 reductase and MDR1/P-glycoprotein. *Pharmaceutical Research*, 2000. 17(7): p. 803-10.
- [48] Benet, L.Z., C.L. Cummins, and C.Y. Wu, Unmasking the dynamic interplay between efflux transporters and metabolic enzymes. *International Journal of Pharmaceutics*, 2004. 277(1-2): p. 3-9.
- [49] Schmiedlin-Ren, P., K.E. Thummel, J.M. Fisher, M.F. Paine, K.S. Lown, and P.B. Watkins, Expression of enzymatically active CYP3A4 by Caco-2 cells grown on extracellular matrix-coated permeable supports in the presence of 1 α ,25-dihydroxyvitamin D₃. *Molecular Pharmacology*, 1997. 51(5): p. 741-54.
- [50] Shiau, Y.F., P. Fernandez, M.J. Jackson, and S. McMonagle, Mechanisms maintaining a low-pH microclimate in the intestine. *American Journal of Physiology*, 1985. 248(6 Pt 1): p. G608-17.
- [51] Lucas, M.L., W. Schneider, F.J. Haberich, and J.A. Blair, Direct measurement by pH-microelectrode of the pH microclimate in rat proximal jejunum. *Proceedings of the Royal Society of London. Series B, Containing papers of a Biological character. Royal Society (Great Britain)*, 1975. 192(1106): p. 39-48.
- [52] Yamashita, S., T. Furubayashi, M. Kataoka, T. Sakane, H. Sezaki, and H. Tokuda, Optimized conditions for prediction of intestinal drug permeability using Caco-2 cells. *European Journal of Pharmaceutical Sciences*, 2000. 10(3): p. 195-204.
- [53] Wikman, A., J. Karlsson, I. Carlstedt, and P. Artursson, A drug absorption model based on the mucus layer producing human intestinal goblet cell line HT29-H. *Pharmaceutical Research*, 1993. 10(6): p. 843-52.
- [54] Hilgendorf, C., H. Spahn-Langguth, C.G. Regardh, E. Lipka, G.L. Amidon, and P. Langguth, Caco-2 versus Caco-2/HT29-MTX co-cultured cell lines: permeabilities via diffusion, inside- and outside-directed carrier-mediated transport. *Journal of Pharmaceutical Sciences*, 2000. 89(1): p. 63-75.
- [55] Artursson, P., A.L. Ungell, and J.E. Lofroth, Selective paracellular permeability in two models of intestinal absorption: cultured monolayers of human intestinal epithelial cells and rat intestinal segments. *Pharmaceutical Research*, 1993. 10(8): p. 1123-9.

-
- [56] Tavelin, S., V. Milovic, G. Ocklind, S. Olsson, and P. Artursson, A conditionally immortalized epithelial cell line for studies of intestinal drug transport. *Journal of Pharmacology and Experimental Therapeutics*, 1999. 290(3): p. 1212-21.
- [57] Avdeef, A., Leakiness and size exclusion of paracellular channels in cultured epithelial cell monolayers-interlaboratory comparison. *Pharmaceutical Research*, 2010. 27(3): p. 480-9.
- [58] Le Ferrec, E., C. Chesne, P. Artusson, D. Brayden, G. Fabre, P. Gires, F. Guillou, M. Rousset, W. Rubas, and M.L. Scarino, In vitro models of the intestinal barrier. The report and recommendations of ECVAM Workshop 46. European Centre for the Validation of Alternative methods. *Alternatives to Laboratory Animals : ATLA*, 2001. 29(6): p. 649-68.
- [59] Zucco, F., A.F. Batto, G. Bises, J. Chambaz, A. Chiusolo, R. Consalvo, H. Cross, G. Dal Negro, I. de Angelis, G. Fabre, F. Guillou, S. Hoffman, L. Laplanche, E. Morel, M. Pincon-Raymond, P. Prieto, L. Turco, G. Ranaldi, M. Rousset, Y. Sambuy, M.L. Scarino, F. Torreilles, and A. Stamatii, An inter-laboratory study to evaluate the effects of medium composition on the differentiation and barrier function of Caco-2 cell lines. *Alternatives to Laboratory Animals : ATLA*, 2005. 33(6): p. 603-18.
- [60] Hayeshi, R., C. Hilgendorf, P. Artursson, P. Augustijns, B. Brodin, P. Dehertogh, K. Fisher, L. Fossati, E. Hovenkamp, T. Korjamo, C. Masungi, N. Maubon, R. Mols, A. Mullertz, J. Monkkonen, C. O'Driscoll, H.M. Oppers-Tiemissen, E.G. Ragnarsson, M. Rooseboom, and A.L. Ungell, Comparison of drug transporter gene expression and functionality in Caco-2 cells from 10 different laboratories. *European Journal of Pharmaceutical Sciences*, 2008. 35(5): p. 383-96.
- [61] Hubatsch, I., E.G. Ragnarsson, and P. Artursson, Determination of drug permeability and prediction of drug absorption in Caco-2 monolayers. *Nature Protocols*, 2007. 2(9): p. 2111-9.
- [62] Motz, S.A., Combined assessment of dissolution and epithelial permeability of solid oral dosage forms, in Department of Biopharmaceutics and Pharmaceutical Technology. 2007, Saarland University: Saarbrücken.
- [63] Ginski, M.J. and J.E. Polli, Prediction of dissolution-absorption relationships from a dissolution/Caco-2 system. *International Journal of Pharmaceutics*, 1999. 177(1): p. 117-25.
- [64] Kobayashi, M., N. Sada, M. Sugawara, K. Iseki, and K. Miyazaki, Development of a new system for prediction of drug absorption that takes into account drug dissolution and pH change in the gastro-intestinal tract. *International Journal of Pharmaceutics*, 2001. 221(1-2): p. 87-94.
- [65] Kataoka, M., Y. Masaoka, Y. Yamazaki, T. Sakane, H. Sezaki, and S. Yamashita, In vitro system to evaluate oral absorption of poorly water-soluble drugs: simultaneous analysis on dissolution and permeation of drugs. *Pharmaceutical Research*, 2003. 20(10): p. 1674-80.
- [66] Ruzicka, J. and E.H. Hansen, Flow injection analyses. Part I. A new concept of fast continuous flow analysis. *Analytica Chimica Acta*, 1975. 78(1): p. 145-157.
- [67] Lindenberg, M., S. Kopp, and J.B. Dressman, Classification of orally administered drugs on the World Health Organization Model list of Essential Medicines according to the biopharmaceutics classification system. *European Journal of Pharmaceutics and Biopharmaceutics*, 2004. 58(2): p. 265-78.

References

- [68] Pade, V. and S. Stavchansky, Link between drug absorption solubility and permeability measurements in Caco-2 cells. *Journal of Pharmaceutical Sciences*, 1998. 87(12): p. 1604-7.
- [69] Rege, B.D., L.X. Yu, A.S. Hussain, and J.E. Polli, Effect of common excipients on Caco-2 transport of low-permeability drugs. *Journal of Pharmaceutical Sciences*, 2001. 90(11): p. 1776-86.
- [70] Troutman, M.D. and D.R. Thakker, Rhodamine 123 requires carrier-mediated influx for its activity as a P-glycoprotein substrate in Caco-2 cells. *Pharmaceutical Research*, 2003. 20(8): p. 1192-9.
- [71] Lindmark, T., Y. Kimura, and P. Artursson, Absorption enhancement through intracellular regulation of tight junction permeability by medium chain fatty acids in Caco-2 cells. *Journal of Pharmacology and Experimental Therapeutics*, 1998. 284(1): p. 362-369.
- [72] Sakai, M., T. Imai, H. Ohtake, H. Azuma, and M. Otagiri, Effects of absorption enhancers on the transport of model compounds in Caco-2 cell monolayers: Assessment by confocal laser scanning microscopy. *Journal of Pharmaceutical Sciences*, 1997. 86(7): p. 779-785.
- [73] Duizer, E., A.H. Penninks, W.H. Stenhuis, and J.P. Groten, Comparison of permeability characteristics of the human colonic Caco-2 and rat small intestinal IEC-18 cell lines. *Journal of Controlled Release*, 1997. 49(1): p. 39-49.
- [74] Imai, T., M. Sakai, H. Ohtake, H. Azuma, and M. Otagiri, In vitro and in vivo evaluation of the enhancing activity of glycyrrhizin on the intestinal absorption of drugs. *Pharmaceutical Research*, 1999. 16(1): p. 80-86.
- [75] Matter, K. and M.S. Balda, Functional analysis of tight junctions. *Methods*, 2003. 30(3): p. 228-34.
- [76] Gumbiner, B., Structure, biochemistry, and assembly of epithelial tight junctions. *American Journal of Physiology*, 1987. 253(6 Pt 1): p. C749-58.
- [77] Powell, D.W., Barrier function of epithelia. *American Journal of Physiology*, 1981. 241(4): p. G275-88.
- [78] Staehelin, L.A., T.M. Mukherjee, and A.W. Williams, Freeze-etch appearance of the tight junctions in the epithelium of small and large intestine of mice. *Protoplasma*, 1969. 67(2-3): p. 165-184.
- [79] Miller, F., Hemoglobin absorption by the cells of the proximal convoluted tubule in mouse kidney. *The Journal of biophysical and biochemical cytology*, 1960. 8: p. 689-718.
- [80] Reuss, L., Tight junction permeability to ions and water, in *Tight Junctions*, M. Cereijido, Editor. 1992, CRC Press: Boca Raton. p. 49-66.
- [81] Schneeberger, E.E. and R.D. Lynch, The tight junction: A multifunctional complex. *American Journal of Physiology - Cell Physiology*, 2004. 286(6 55-6): p. 1213-1228.
- [82] Angelow, S., R. Ahlstrom, and A.S.L. Yu, Biology of claudins. *American Journal of Physiology - Renal Physiology*, 2008. 295(4): p. 867-876.
- [83] Hidalgo, I.J., Assessing the absorption of new pharmaceuticals. *Current Topics in Medicinal Chemistry*, 2001. 1(5): p. 385-401.
- [84] Wegener, J., D. Abrams, W. Willenbrink, H.-J. Galla, and A. Janshoff, Automated multi-well device to measure transepithelial electrical resistances under physiological conditions. *BioTechniques*, 2004. 37(4): p. 590-597.

-
- [85] Steimer, A., E. Haltner, and C.-M. Lehr, Cell culture models of the respiratory tract relevant to pulmonary drug delivery. *Journal of Aerosol Medicine: Deposition, Clearance, and Effects in the Lung*, 2005. 18(2): p. 137-182.
- [86] Riley, S.A., G. Warhurst, P.T. Crowe, and L.A. Turnberg, Active hexose transport across cultured human Caco-2 cells: Characterisation and influence of culture conditions. *Biochimica et Biophysica Acta (BBA) - Biomembranes*, 1991. 1066(2): p. 175-182.
- [87] Artursson, P., A.-L. Ungell, and J.-E. Lofroth, Selective paracellular permeability in two models of intestinal absorption: Cultured monolayers of human intestinal epithelial cells and rat intestinal segments. *Pharmaceutical Research*, 1993. 10(8): p. 1123-1129.
- [88] Lu, S., A.W. Gough, W.F. Bobrowski, and B.H. Stewart, Transport properties are not altered across Caco-2 cells with heightened TEER despite underlying physiological and ultrastructural changes. *Journal of Pharmaceutical Sciences*, 1996. 85(3): p. 270-273.
- [89] Adson, A., T.J. Raub, P.S. Burton, C.L. Barsuhn, A.R. Hilgers, K.L. Audus, and N.F. Ho, Quantitative approaches to delineate paracellular diffusion in cultured epithelial cell monolayers. *Journal of Pharmaceutical Sciences*, 1994. 83(11): p. 1529-36.
- [90] Finley, J.W. and P. Monroe, Mn absorption: The use of CACO-2 cells as a model of the intestinal epithelia. *Journal of Nutritional Biochemistry*, 1997. 8(2): p. 92-101.
- [91] Davis, S.S., J.G. Hardy, and J.W. Fara, Transit of pharmaceutical dosage forms through the small intestine. *Gut*, 1986. 27(8): p. 886-892.
- [92] Cereijido, M., E.S. Robbins, W.J. Dolan, C.A. Rotunno, and D.D. Sabatini, Polarized monolayers formed by epithelial cells on a permeable and translucent support. *Journal of Cell Biology*, 1978. 77(3): p. 853-80.
- [93] Martinez-Palomo, A., I. Meza, G. Beaty, and M. Cereijido, Experimental modulation of occluding junctions in a cultured transporting epithelium. *Journal of Cell Biology*, 1980. 87(3 Pt 1): p. 736-45.
- [94] Noach, A.B.J., Y. Kurosaki, M.C.M. Blom-Roosemalen, A.G. de Boer, and D.D. Breimer, Cell-polarity dependent effect of chelation on the paracellular permeability of confluent caco-2 cell monolayers. *International Journal of Pharmaceutics*, 1993. 90(3): p. 229-237.
- [95] Watson, C.J., M. Rowland, and G. Warhurst, Functional modeling of tight junctions in intestinal cell monolayers using polyethylene glycol oligomers. *American Journal of Physiology - Cell Physiology*, 2001. 281(2 50-2): p. 388-397.
- [96] Yap, A.S., J.M. Mullin, and B.R. Stevenson, Molecular analyses of tight junction physiology: Insights and paradoxes. *Journal of Membrane Biology*, 1998. 163(3): p. 159-167.
- [97] Konishi, Y., K. Hagiwara, and M. Shimizu, Transepithelial Transport of fluorescein in Caco-2 cell monolayers and use of such transport in in vitro evaluation of phenolic acid availability. *Bioscience, Biotechnology and Biochemistry*, 2002. 66(11): p. 2449-2457.
- [98] Kuwayama, K., S. Miyauchi, R. Tateoka, H. Abe, and N. Kamo, Fluorescein uptake by a monocarboxylic acid transporter in human intestinal Caco-2 cells. *Biochemical Pharmacology*, 2002. 63(1): p. 81-88.